IMPROVED DISEASE MANAGEMENT OF HEART FAILURE PATIENTS USING THE PULSE WAVE VELOCITY METHODOLOGY

University of Coimbra

Faculty of Sciences and Technology

Dissertation

Integrated Masters in Biomedical Engineering

Jorge Daniel Leonardo Proença

2009/2010

Dissertation submitted to the University of Coimbra to fulfill the requirements for the degree of Master in Biomedical Engineering

Supervisors:

Jens Muehlsteff
Philips Research Aachen

Paulo de Carvalho
Department of Informatics Engineering (DEI)
Faculty of Sciences and Technology of University of Coimbra (FCTUC)

Acknowledgements

I would like to present my greatest gratitude to both my supervisors, Paulo de Carvalho and Jens Muehlsteff, for their guidance throughout the project which was invaluable and for their constant availability and regular teleconferences (‘telcos’) that kept everyone connected.

I am also thankful for the help of the signal processing group of DEI, for providing the superb point detection alghoritms that made my work a little bit easier.

I am very grateful to Mr. Xavier Aubert from Philips Research Aachen for his collaboration on the produced conference paper and his precious help on making sense of the Moens-Korteweg equation origins.

A big ‘thank you’ to all my friends and colleagues in Aachen that contributed to me feeling welcome for my 4 month stay in Germany. You will be missed.

Finally, I dedicate this work to my family and friends in Portugal, for always being there.

Abstract

Cardiovascular diseases (CVD) are a major cause of death globally and there are a lot of expense concerns associated. Heart failure (HF) is the CVD with the most incidences and is characterized by the heart not pumping enough blood to the body. The importance of non-invasive and continuous solutions for personal health systems is in ascension, and this project deals with investigating markers in the cardiovascular system of a subject to help improve management of HF and evaluating therapeutic effects.

This work investigates healthy young subjects during a sequence of short-term physical exercises. Blood pressure (BP) is a very important marker of the cardiovascular system and the Pulse Transit Time (PTT) is generally assumed to be a good surrogate measure to comfortably track BP and BP changes. PTT was measured by two different methodologies having different accuracies and underlying assumptions: the total PTT from heart to fingertip and the difference of fingertip and earlobe PTTs (DPTT). Low correlations with systolic blood pressure (SBP) have been observed and in conclusion, there might be a need for an improved measurement accuracy of the techniques in use. The applicability of the Moens-Korteweg (M-K) equation is also questionable for young people having flexible arteries as significant radius changes (excluded from the M-K model) occur in the large arteries during exercise, which might counteract a PTT decrease with the BP elevation.

Heart Rate and Pulse arrival time are also evaluated as they exhibit interesting changes with physical exercise. These are modeled separately and exhibit similar patterns when analyzed together. It is foreseen that changes or abnormalities in the cardiovascular system in diseased subjects may disrupt the regular patterns, and easy evaluations can be extrapolated. Proposed future work involves moving to data from actual diseased patients.

Resumo

As doenças Cardiovasculares (DCV) são a maior causa de morte mundialmente e existe muita preocupação de custos associados. A Insuficiência Cardíaca (IC) é uma das DCV mais incidentes e é caracterizada por o coração não bombear sangue suficiente para o corpo. A importância de métodos não invasivos e contínuos para sistemas de saúde pessoal está em ascensão e este projecto lida com o investigar de marcadores no sistema cardiovascular de um sujeito que ajudem a melhorar a gestão de IC e avaliar os efeitos terapêuticos.

Este trabalho investiga sujeitos jovens e saudáveis durante uma sequência de exercícios físicos de curto prazo. A pressão sanguínea (BP) é um importante marcador do sistema cardiovascular e o tempo de trânsito de pulso (PTT) é geralmente assumido como uma boa medida para seguir confortavelmente a BP e mudanças na BP. PTT foi medido com dois princípios diferentes: PTT total do coração ao dedo da mão e diferença de PTTs do dedo e ouvido. Foram observadas baixas correlações com BP sistólica e em conclusão serão necessário métodos mais precisos. A aplicabilidade da equação de Moens-Korteweg (M-K) também é questionável para sujeitos jovens que têm artérias flexíveis pois mudanças de raio (excluídas no modelo de M-K) ocorrem nas artérias grandes durante o exercício, o que pode contra-agir uma diminuição de PTT com a elevação de BP.

O ritmo cardíaco e tempo de chegada de pulso são também avaliados pois exibem mudanças interessantes com exercício físico. Estes são modelados separadamente e exibem padrões semelhantes quando analisados conjuntamente. É previsto que mudanças ou anormalidades no sistema cardiovascular em pacientes debilitados possam dar origem a padrões diferentes dos regulares, e uma fácil avaliação poderá ser extrapolada. A proposta de trabalho futuro envolve passar para dados de pacientes com doença.

Contents

List of Figures

List of Tables

Acronyms

CVD	Cardiovascular Diseases
CV	Cardiovascular
HF	Heart Failure
CHF	Congestive Heart Failure
PTT	Pulse Transit Time
PAT	Pulse Arrival Time
PEP	Pre-ejection Period
BP	Blood Pressure
SBP	Systolic Blood Pressure
DBP	Diastolic Blood Pressure
ECG	Electrocardiogram
PPG	Photopletismogram
ICG	Impedance cardiogram
HR	Heart Rate
M-K	Moens-Korteweg
AVG	Average
STD	standard deviation

1. Introduction

1.1. Motivation

Cardiovascular diseases (CVD) are the major cause of death globally and are prompted as a major concern for healthcare expenses. According to the European Heart Network they account for 2.0 million deaths/year in the European Union (EU) and an expenditure of €192 billion per year as of 2008 [1]. Chronic diseases in general account for 60% of deaths worldwide [2]. Heart failure (HF) is a condition where the heart is not pumping the sufficient amount of blood the body needs and there are an estimate of 10 million patients with Heart Failure in the EU. The uprising implementation of Personal health systems is directly related to the importance in finding non-invasive monitoring solutions to improve patient disease management, helping in the recovery process and medication intake, and avoid or shorten expensive hospital stays.

The HeartCycle project – 'Compliance and effectivness in heart failure and coronary heart disease (CHD) closed-loop management' – funded by the EU and with 18 partners from research, academic, industrial and medical organizations, is lead by Philips. The main objective is to develop systems to monitor remotely patients with HF and CHD that motivate the patient to comply with treatment and regimes. Furthermore, there is a need to optimize the evaluation of health status and impact of current medication using vital body signs and others measurements.

To have blood pressure (BP) measures would be crucial, being an important marker of the cardiovascular system and whose behavior relates deeply to CV problems. Its beat-to-beat (continuous) monitoring has a high prognostic and diagnostic value. But the "gold standard" for arterial BP non-invasive measurement is the conventional cuff-based mercury sphygmomanometer which may provide many false readings for home-monitoring. Non-invasive continuous solutions would highly benefit from an easy and complication-free way towards BP monitoring. Along this line, Pulse Wave Velocity (PWV) or the inverse Pulse Transit Time (PTT) have been identified as promising surrogate parameters for comfortable and continuous BP monitoring.

1.2. Project Overview

This academic project is of an investigative and speculative nature. It involves mostly signal processing and theoretical evaluations. Work environments were the Department of Informatics Engineering (DEI) and Philips Research in Aachen, Germany.

The analysis of Pulse Transit Time culminated on a paper for the EMBC conference of 2010 titled 'Is Pulse Transit Time a good indicator of Blood Pressure changes during short physical exercise in a young population?', annexed.

1.3. Objectives

The initial and main objective was to investigate pulse wave velocity/ pulse transit time related measures and markers in patient cardiovascular/hemodynamic status to improve congestive heart failure management. It would be very useful in this setting if found that adding PWV or the inverse Pulse Transit Time PTT as a measurement for the system would help in condition assessment. With the unpredictability of not having heart-failure data during the project duration, all of the results relate to behaviors of healthy subjects performing physical efforts. Nevertheless, predictions are made on what may happen for sick subjects and all of the work still had the initial objective in mind.

Specific objectives are:

- Evaluate PTT as a surrogate parameter for tracking BP and BP changes in a continuous and non-invasive way;
- Appraise the limitations of the calibration model of getting BP from PTT;
- Explore the variations of HR and PAT in physical exercise and deviations to the existent patterns as indicators of heart condition and action of regulation mechanisms;
- Explore the predictability of HR and PAT variations by modeling them independently;
- Investigate possible applications of physical exercise trials with PTT related measuring.

1.4. Report Structure

This document is divided into six main chapters. After this introduction comes a chapter with the relevant theoretical background captured throughout the project on the cardiovascular system and its features, regulation mechanisms and state-of-the-art. The dataset and signals chapter describes the inherent protocol behind the analyzed research data along with the depiction of the signals extracted, the noise filtering applied and base-line processing and variable estimation.

The two central chapters follow, which separate two distinct premises. These chapters introduce the main methods for the related modeling and analysis associated with the different physiological parameters, the main achieved results and their discussion. Chapter entitled ‘Methodology of Pulse Transit Time’ gathers PTT associated findings, exploring thoroughly the topics that lead to the conference paper produced – calibration to get blood pressure through PTT or difference of PTT, sensitivities associated and accuracy of measurements. The subsequent chapter entitled ‘Heart Rate and Pulse Arrival Time in physical exercise’ concerns the investigation of variation trends in these two physiological parameters during exercise and recovery periods. These trends provide indications on the condition of the heart and on the behavior of regulatory mechanisms.

In the last chapter, the main conclusions are exposed as well as proposals for future work and applications. At the end of the document, a set of annexes present in a systematic way all the tables of values mentioned throughout the text as well as individual cases. Detailed proofs of the proposed models are also introduced in these annexes.

2. Background

2.1. Cardiovascular system physiological aspects

2.1.1. The Heart

The heart has a vital role as a functional and maintenance organ of the human body. It is the pump of the circulatory system, where it enables the travelling of blood (the transport medium) to the vicinity of every living tissue in the organism through the blood vessels (the delivery route). Blood, among other regulatory and protective functions, provides the necessary distribution of oxygen from the lungs and nutrients from the digestive tract to all body cells as well as carrying waste from these cells to be eliminated (carbon dioxide through the lungs and other wastes through the kidneys).

Fist-sized, the heart has four chambers (two atria and two ventricles) which constitute two different sides each one with its input and output of blood (Fig. 1). Muscle walls – the myocardium – surround these chambers and, by contracting, are responsible for the movement and pumping of blood in the heart. These contractions are based on electrical depolarization which is intrinsic to heart (does not need external stimulation). However, it is connected to the autonomic nervous system which can alter the basic rhythm of heart activity. Certain hormones also take effect in heart regulation.

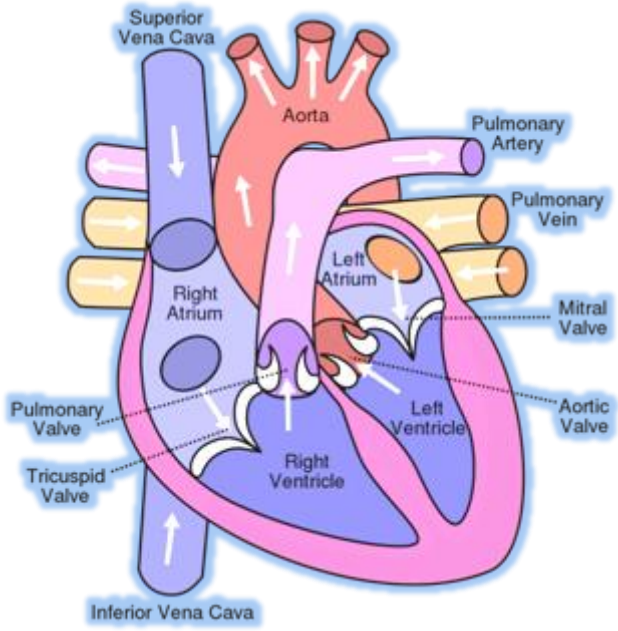

Figure 1 – Schematic of heart constitution. Adapted from [3]

2.1.2. Circulation

There are two main types of blood vessels: arteries that carry blood away from the heart, and veins that collect and return it. The arterial tree starts with the aorta, the thickest of arteries, at the exit of left ventricle (aortic valve) and the branching arteries progressively diminish in radius size until they become capillaries. Arteries are generally very elastic, stretching to the

passage of the cardiac-originated pressure stimuli (compliance) and major arteries are the most compliant. Veins are subject to lower pressures; therefore their walls are thinner than arteries and sometimes valves are present to prevent the backflow of blood.

The double-sided nature of the heart indicates two separate circulations: Pulmonary and Systemic circulation (Fig.2).

Pulmonary Circulation

Oxygen-poor blood is pushed from the right ventricle to the pulmonary arteries, reaching the lungs where the gaseous exchanges occur. Oxygen is diffused from alveolus into the capillaries and carbon dioxide is expelled. Pulmonary veins then carry the oxygen-rich blood back to the heart, where it enters at the left atrium.

Systemic Circulation

Between contractions, the left ventricle is continuously filled from the left atrium, passing through the left Atrioventricular (A-V) valve (as known as mitral valve). When it contracts, mitral valve closes to prevent backflow to the atrium and aortic valve opens moments later, setting the blood which is now rich in oxygen on a path through the aorta, which branches out, supplying the entire body. After blood has been to the capillary beds of all tissues, it is carried back in veins which ultimately join in the superior and inferior vena cava, ending in the right atrium of the heart.

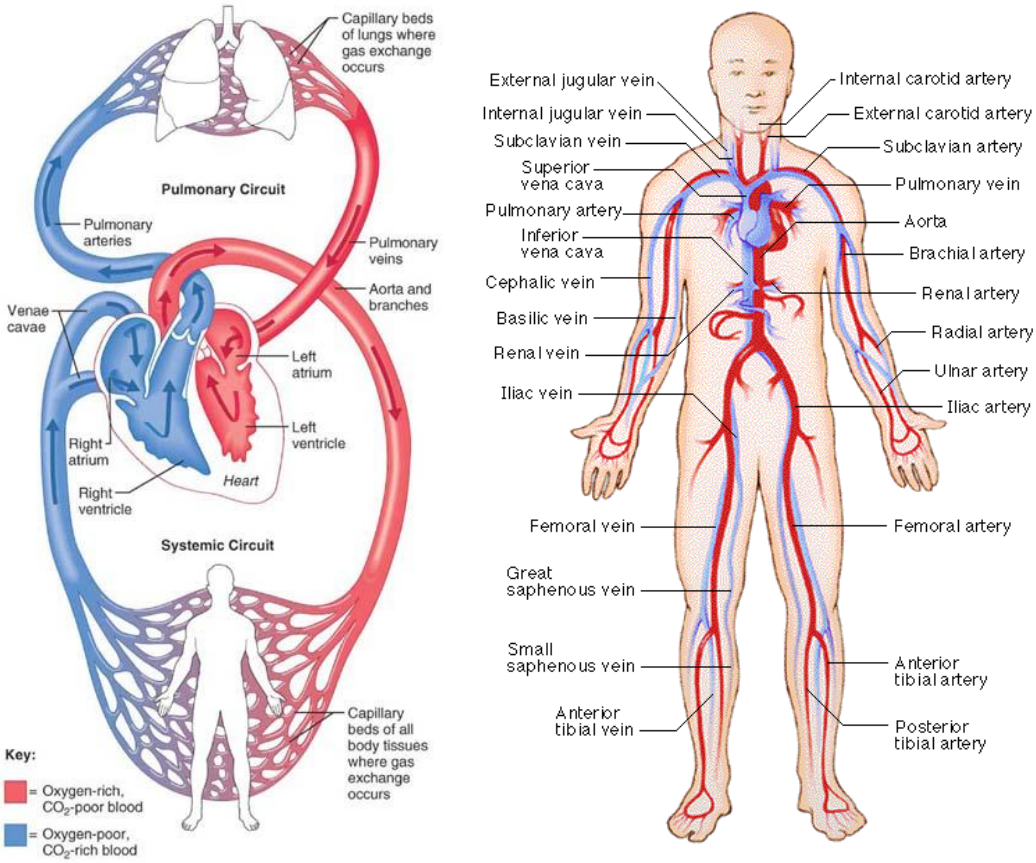

Figure 2 – Schematic of systemic and pulmonary circulations (left, [6]) and overview of the vessels of the circulatory system (right, [4]).

2.2. *Time-intervals and blood pressure*

Figure 3 depicts the events for two cardiac cycles, where one can see the connections between atrial, ventricular and aortic pressure along with ejection and refill periods of the ventricle. Ventricular systole is the period in which the ventricles are contracting and the complementary diastole refers to a relaxed state of the ventricles.

The Pre-ejection period (PEP) is defined as the time interval from the start of ventricular depolarization (marked by the beginning of the QRS complex in the ECG) which leads do ventricular contraction to the start of ejection of blood (marked by aortic valve opening). Therefore it includes excitation-contraction coupling (converting electrical stimulus to mechanical response) and the isovolumetric contraction phase (ventricle starts to contract but aortic valve only opens after ventricular pressure exceeds aortic pressure).

Left ventricle ejection time (LVET) is the ejection period itself, which immediately follows PEP and ends with the closing of aortic valve.

A healthy heart usually has a short PEP and a long LVET meaning a high contraction efficiency or contractility. Lower aortic pressure also helps to lower the PEP and increase LVET as it is equaled earlier by ventricular pressure. The PEP/LVET index (dividing PEP by LVET) has been researched as an indicator of heart function and contractility although the index values may vary substantially, seemingly due to heart rate and blood pressure.

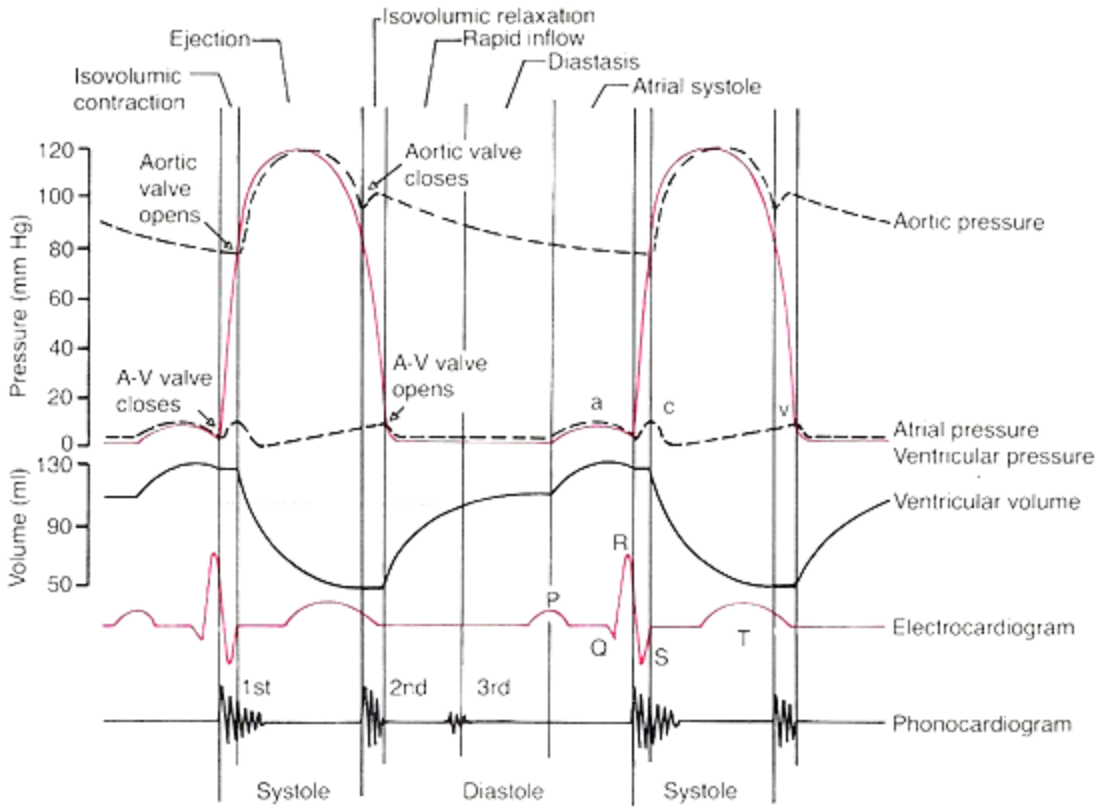

Figure 3 - Events of the cardiac cycle [5]

Due to the contraction of the left ventricle and ejection of blood, a pulse wave originating in the aortic arch propagates with pressure, volume and flow. Blood pressure (BP) then relates to the force exerted to the arterial walls by the passing blood, with Diastolic Blood Pressure (DBP) being corresponding to an idle period and Systolic Blood Pressure (SBP) being the peak pressure value at passage of the pressure pulse (fig. 4). The Mean Arterial Pressure (MAP) can normally be extrapolated from these two (MAP ≈ *DBP+(SBP-DBP)/3*).

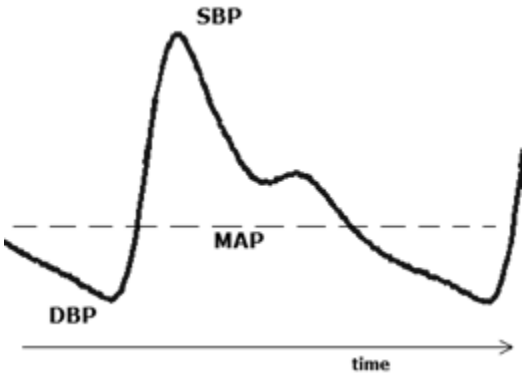

Figure 4 – Typical pressure wave in an artery

Pulse Transit Time (PTT) corresponds to the duration of the pressure pulse to propagate through a segment of the arterial tree, usually until an extremity, and it's indicative of the velocity in which the pulse flows through that segment (PWV):

$$PWV = \frac{\text{distance}}{PTT} \tag{2.1}$$

In this project, seeing as PTT values are related to periphery measures, different arteries are involved in the pathway considered that starts in the aorta. PWV may change along this path, therefore PTT and PTT changes can only describe average PWVs. This is the reason why PTT is addressed more intensively in this study than PWV, also due to path distances not being always available. In general, PTT is in the order of 150-200 ms, and e.g., considering an arm length of 1 meter, PWV would be 6.7-10 m/s.

Arterial Stiffness, which increases with age, is characterized by a diminishing diameter of the vessels which provokes alterations in PWV and PTT, and is also one of the main diagnostic parameters estimations of pulse wave velocity, especially in major arteries.

Pulse Arrival Time (PAT) is defined as a broader time-interval that includes PEP and PTT. Therefore:

$$PAT = PEP + PTT \tag{2.2}$$

Often in literature the denomination of transit time/PTT is used for the here depicted PAT. For the simplicity of measuring PAT, not going for opening of aortic valve but for the beginning of contraction, it is then used as a rough approximation of PTT. Nevertheless, for this document, let there be always a clear distinction of PAT and PTT.

2.3. Blood Pressure Regulation Mechanisms

There are three main points of action of cardiovascular and blood pressure regulation mechanisms. These are: affecting Cardiac Output by changing heart rate, contractility and stroke volume; vessel control such as vasoconstriction and vasodilation of the arteries; and long term mechanisms affecting blood volume (retaining or expelling water through the kidneys).

To maintain a steady flow of blood from the heart to the extremities is essential for correct organ function. Moreover, making sure that a person standing up from a lying down position gets adequate blood flow to the brain requires precise cooperation of the heart, blood vessels, and kidneys, all of these with the supervision of the brain. The most crucial of regulation mechanisms of cardiovascular dynamics, are the ones that maintain blood pressure, mainly cardiac output, blood volume and peripheral resistance.[6]

Regulation mechanisms can affect pressure both in the short-term and long-term. Short-term mechanisms usually involve a change in sympathetic and parasympathetic activity, changing cardiac output and peripheral resistance. Long-term regulation involves renal regulation of blood volume via the renin-angiotensin and aldosterone mechanisms [7].

Short-Term Mechanisms

When arterial blood pressure rises, it stretches baroreceptors, neural receptors located in the carotid sinuses (dilations in the internal carotid arteries, which provide the major blood supply to the brain), in the aortic arch, and in the walls of nearly every large artery of the neck and thorax. When stretched, baroreceptors send a rapid stream of impulses to the brain that provoke increased activity of parasympathetic nerves (vagus nerves) and decreased sympathetic activity. This leads to a reduction of heart rate, which induces less cardiac output, and relaxation of vascular smooth muscle, that causes an increased arterial diameter. These promote the lowering of blood pressure.

On the other hand, for falling blood pressure, the baroreceptors are inhibited and send fewer impulses to the brain, causing a decrease in parasympathetic activity and an increase in sympathetic activity. The increased activity of sympathetic nerves acts on three fronts. The first one is the increase heart rate and contractility that cause and higher cardiac output and therefore higher blood pressure. The second is the increased constriction of va scular smooth muscle and decreases arterial diameter to increase peripheral resistance and blood pressure. The third is the effect of the sympathetic activity on adrenal glands. More commonly if a period of stress occurs, the adrenal gland releases norepinephrine and epinephrine to the bloodstream, hormones that enhance the sympathetic response. Norepinephrine has a vasoconstrictive action, while epinephrine promotes generalized vasoconstriction (except in skeletal and cardiac muscle) and increases heart rate and contractility. This effect is slower-acting and a bit more prolonged than the direct nervous control.

There are more hormone control mechanisms for short-term effects on blood pressure. For example, Atrial natriuretic peptide (ANP) produced by the atria of the heart, causes generalized vasoconstriction. It also inhibits aldosterone and renin secretion, and decreases sodium and water reabsorption in the kidneys, leading to a drop in blood volume. Angiotensin, generated by renin, and involved in long-term regulation mechanisms, also stimulates intense vasoconstriction, promoting a rapid rise in systemic blood pressure.

Long-Term Mechanisms

Although baroreceptors respond to short-term changes in blood pressure, they quickly adapt to prolonged or chronic episodes of high or low pressure. This is where the kidneys step in to restore and maintain blood pressure homeostasis by regulating blood volume. Although blood volume varies with age, body size, and sex, renal mechanisms usually maintain it at close to 5 L. The loss of blood through hemorrhage, accident, or donating blood will lower blood pressure and trigger processes to restore blood volume back to normal.

The kidneys act both directly and indirectly to regulate arterial pressure and provide the major long-term mechanism of blood pressure control. The direct renal mechanism alters blood volume independently of hormones. When either blood volume or blood pressure rises, the rate at which fluid filters from the bloodstream into the kidney tubules is speeded up. In such situations, the kidneys cannot process the filtrate rapidly enough, and more of it leaves the body in urine. As a result, blood volume and blood pressure fall. When blood pressure or blood volume is low, water is conserved and returned to the bloodstream, and blood pressure. As blood volume goes, so goes the arterial blood pressure.

The indirect renal mechanism is the renin-angiotensin mechanism. When arterial blood pressure declines, the kidneys release the enzymatic hormone renin into the blood. Renin triggers a series of reactions that produce angiotensin II, as mentioned previously. Angiotensin II is a potent vasoconstrictor, increasing blood pressure by increasing peripheral resistance. It also stimulates the adrenal cortex to secrete aldosterone, a hormone that enhances renal reabsorption of sodium. As sodium moves into the bloodstream, water follows; thus, both blood volume and blood pressure rise. Aldosterone and increased blood osmolarity also cause the posterior pituitary to release antidiuretic hormone (ADH), which promotes more water reabsorption, and excites the thirst center, also resulting in higher blood volume and pressure.

2.4. Physical Exercise effects on the CV system

Long term regulation mechanisms should not be observable for short physical efforts, although blood volume changes would be an important marker in congestive heart failure, also for often used medications such as diuretics.

Physical exercise induces several changes in the cardiovascular system. With it, the working muscles and tissues need an increased level of oxygen and nutrients and the body adapts the cardiorespiratory system to correspond to this need. Breathing rate increases to increase oxygen intake and the heart will contract faster and stronger to increase blood flow to

the tissues. There are also significant changes in small blood vessels, for different regions of the body, consequently shifting blood flow to the active muscles. Another way to approach physical exercise changes and regulation is stating that the body accepts a higher value of Blood Pressure (BP) and works towards maintaining this new level or set-point.

Increased Sympathetic activity of the Autonomic nervous system leads to a raise in Heart Rate (HR) and in the force of each contraction. If only HR increased, there would be less time for ventricular filling and the Stroke Volume (SV) should be lower, but, due to improved contractility, less blood is left at the end of contraction (end systolic volume decreases) and the SV does not decrease profoundly. Also, the squeezing action of the skeletal muscles on the veins returning blood to the heart leads to a higher end diastolic volume, and so the SV increases (there's an increase in venous return, also due to the higher heart rate). All of this contributes to the intended raise of Cardiac Output (CO; the combination of Heart Rate and Stroke Volume), and there's a higher and more frequent supply of blood from the heart:

$$CO = SV \times HR \tag{2.1}$$

Note: Appended (7.2.2) is a table where the variations of cardiac values are presented for the project's dataset of healthy young subjects in short physical exercises. In average there are max variations in Heart Rate of 66–115 beats/min, Stroke Volume of 72–111 ml and Cardiac Output of 5.66–11.01 L/min. The time-scale involved is of approximately 1 minute to reach the highest HR state from the beginning of each exercise run.

In active muscles, metabolism increases and the consequent decrease of oxygen concentration and accumulation of metabolic factors lead to a phenomenon called exercise hyperemia. This autoregulation is characterized by an increase of blood flow in direct proportion to the level of metabolic activity of the muscles. The vasomotor center must also induce systemic changes to guarantee that there is a faster and more abundant delivery of blood to the muscles and during exercise there is an increase of nervous system sympathetic activity. Vessels in other organs such as the digestive viscera, which make up great blood reservoirs, suffer from vasoconstriction due to sympathetic action and blood is diverted temporarily from these regions to ensure a bigger delivery to the working muscles. In the skeletal muscles, local controls override the sympathetic commands of vasoconstriction and the opposite effect occurs (vasodilation). With all this, the increase of cardiac output and the dilation of practically all capillaries in the active muscles, a significant increase in blood flow for skeletal muscles is achieved. [6]

2.5. State-of-the-art

2.5.1. Non-invasive BP measurement

The most precise methods of obtaining blood pressure (BP) are invasive techniques, used most commonly in hospitals in intensive care units, where a procedure is necessary to get a direct measurement in the arteries, which always carries a certain risk. These are definitely not

applicable for non-hospital scenarios and non-invasive methods are the appropriate solution for check-up, disease prevention measurements and home-monitoring systems.

The "gold standard" for non-invasive arterial blood pressure measurement is the conventional mercury sphygmomanometer and has been for over 100 years. As a result, the standard units for pressure in medicine and physiology are still millimeters of mercury (mmHg). There are several limitations on using cuff-based methods. The sphygmomanometer auscultatory method depends on the detection of Korotkoff sounds by the examiner [8] and results may vary if the examiner is changed or different inflation is applied. Even the electronic method using the sphygmomanometer and oscillometry [9] can generate inaccurate readings in patients with circulatory or heart problems and many of these equipments have not been clinical validated. Cuff-based methods also don't allow for continuous monitoring of BP, achieved by obtaining measurements for each heart-beat (beat-to-beat). Continuous monitoring is essential when evaluating a patient's cardiovascular status and to follow BP changes through recovery events for physical activity or posture changes. Consequently, there have been several efforts to join continuous with non-invasive methodology and to find ways of extracting blood pressure through surrogate parameters that have a direct or indirect connection to its value and variation. Some of the most popular are:

- Vascular unloading method [10,11], equipments: Finapres, Portapres, Finometer.

- Tonometric method [12]

There is also extensive research on obtaining BP through different methods [13]:

1 – Impedance Cardiography – derived from thorax impedance, it can be obtained non-invasively and can provide information on the incidence of several cardiac events such as atrial and ventricular contraction and opening and closing of aortic valve [14]. Therefore, connection to blood pressure is a possibility and several efforts have been made using this setup.

2 – Heart Sounds – also easily obtainable non-invasively, they have been explored either by time-lapse or intensity as ways of estimating BP. [15,16]

2.5.2. Pulse Transit Time to Blood Pressure

Several studies using the pulse wave velocity (PWV) / pulse transit time (PTT) for cuff-less and non-invasive continuous blood pressure estimations have demonstrated the possibility of obtaining BP from PTT [17,18,19,20,21,22].

There are different setups to obtain a pulse transit time, but the most common include the use of Photoplethysmography (PPG), which gives the perfusion of blood in the skin. Using this procedure a signal describing arterial pulses is obtained. PPG is usually used at an extremity and the instant of arrival of blood related to a systole can be detected through the beginning of a pulse. Then, a Pulse transit time can be obtained by detecting the beginning of ejection of blood through the left ventricle (e.g. through ICG) and getting the difference between this instant and the arrival of the pulse at the location of the PPG. There are alternatives to have a PTT measure, such as using a setup of two PPG signals, e.g., at the finger and the earlobe, where there should be a difference in arrival of pulses and thus a pulse transit time variation can be derived and

analyzed [23,24]. Although this is not the real/true PTT, it eliminates the need for other signals other than PPG, and changes in PTT can be observed.

Studies have shown that posture and physical activity are variables to be considered [25,26] very important in interpreting PAT monitoring in uncontrolled scenarios (home monitoring). When studying the influence of physical activity, it has been determined that PEP is the predominant influence on PAT variations for short physical efforts, with consistent BP alterations. Being so, determination of blood pressure through PTT may not be the best approach in this situation and a generalized PWV related to PAT has been used in, determining a heuristic linear calibration function to estimate SBP.

Hydrostatic pressure has been shown to have a significant effect on PTT and has even been proposed as a calibration approach through hand elevation for PTT-based cuff-less BP measurements.[27,28] Posture changes have a significant subject-specific effect for healthy individuals on PAT at almost constant systolic and diastolic blood pressure. In Muehlsteff et al.[26], PEP and PAT changes that are not consistent with BP variations were observed, due to alterations of the body posture (lying, sitting, and standing). It is proposed that, through individual calibration for each subject, posture effects may be compensated, although the phenomenon could not be fully explained. Through the use of PAT and a sleeping bed, W. B. Gu et al.[29] show considerable changes in BP estimation through PAT when in supine and sitting positions and that new compensation factors must be procured in order to account for posture changes.

There are other methods for dealing with PPG to get Blood pressure, e.g., inferring BP from the amplitude of the arterial volume pulse wave, given by the PPG. There is a known relationship of pressure and volume of elastic arteries and so the amplitude of PPG signal can be strongly coupled to blood pressure. This method is limited when using a PPG signal at an extremity/peripheral vasculature, as microcirculatory autoregulations influence the local pulse wave amplitude due to several factors.

2.5.3. Heart failure management

Congestive Heart failure (CHF) is a condition where a problem with the functioning or structure of the heart weakens its ability to maintain sufficient cardiac output to meet the body's needs. Therefore, congestion of fluids in the systemic circulation occurs. When this inability becomes critically imparing, a decompensation episode occurs. At the first episode of acute decompensated heart failure, which is for 70% of the patients also the time they get diagnosed with the condition, patients get acute treatment in the hospital. This treatment focuses on extracting the excess water from the patient's body through the use of diuretics and on managing the patient's disease through medication. After discharge, the patient often undergoes a phase where the right medication dosage has to be found. Starting from low dosages, the drugs are up titrated over several weeks. After up-titration of medication, the patient then undergoes a stable phase until the condition worsens and he is hospitalized for acute decompensated heart

failure again. Every decompensation that the patient had leaves irreparable damages to the heart and leads to a higher chance of a subsequent hospitalizations.

Disease Management

The main objective of Congestive Heart Failure disease management is to reduce the deterioration of patient condition through close monitoring (with practical application, usually tele-monitoring in unsupervised environments) of related parameters and timely detection of a decompensation event. With this, one can take the necessary steps in treating decompensation earlier, and hospitalization may even be avoided, leading to less aggravation in each episode, better health status recovery, and consequently, a slower progression of the disease.

Several tele-monitoring devices for Health status assessment of Heart Failure patients have been on development[30,31]. In the preceding MyHeart project [32], spectral bioimpedance is the main technique used to evaluate heart failure and attempt early detection of decompensation. In HeartCycle, other approaches will be attempted and studied, including the use of PAT and systolic time-intervals. Medication control is also important and effects of medication in several parameters shall also be explored.

3. *Dataset and Signals*

3.1. Setup

The entire project dealt with the study of data from physical exercise trials. The main data-set comes from a previous Philips trial where 20 healthy subjects performed sequential sets of short term efforts in an ergometer cycle following the protocol described in figure 5. Three exercise runs of increased power, 25, 45 and 65W, are performed with 5 minute breaks after each.

Figure 5 – Schematic of exercise protocol of the main study dataset

The study population has the following characteristics (complete table in annex 7.2.1):

- Males/Females: 14 / 6
- Age: 28.8 ± 8.4 years
- Height: 175.3 ± 9.8 cm
- Weight: 69.8 ± 14.3 kg
- Body Mass Index: 22.5 ± 2.8 kg/m2

The relevant extracted signals were:

- 3 lead Electrocardiograph (ECG);
- Photopletismographs (PPG) at three locations: left index finger; left earlobe, forehead;
- Pressure wave and Systolic and Diastolic Blood Pressure values from the Portapres device [33];
- Pre-ejection period obtained through Impedance Cardiogram (ICG) from the Niccomo device [34];
- Breathing effort from a respiration band;
- Movement information from an accelerometer.

Sampling frequency of ECG, PPG and accelerometer were of 200 Hz, while BP values are beat to beat and PEP values are given with a 1Hz frequency. Time stamping is available for every signal so synchronicity is achieved.

3.2. Variable extraction and filtering

Matlab was the tool used to visualize and process data and to perform the several analyses throughout the project. The first issue to deal with was signal noise and outliers which were a common problem, especially within the PEP signal. Motion artifacts may be the main contribution to this noise, being that it is mostly present during exercise periods. Depicted in figure 6a is a typical example (borderline usable) of a noisy PEP signal, centered on an exercise run (with decreasing PEP) where large variations are observable during exercise. However, a trend can be envisioned of where the real values should lie, corresponding in exercise to the lower values, thus stating that the noise is characterized by upward spikes and these outliers are probably due to late misdetections by the Niccomo device. Knowing beforehand that PEP usually decreases for exercise is also an indicator. The outliers are removed using a median filter, by limiting the changes in the signal to a certain interval centered on a level from previous values (the median). This filter is also employed during Heart Rate and PAT estimation to remove outliers. A low-pass filtering is then applied for a smoother PEP signal.

Due to rougher and unusable PEP signals as exemplified in figure 6b, 6 subjects (subjects n. 5, 7, 8, 9, 12 and 14) had to be dropped from analysis as no trend could be extrapolated.

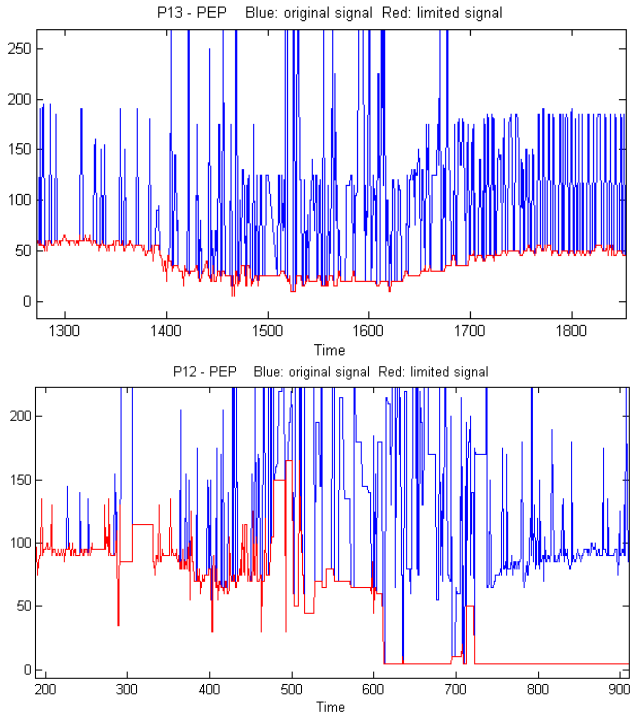

Figure 6 – PEP signal example with noise and median limiting.
5a (top) – borderline usable signal; 5b (bottom) – unusable signal.

3.3. Pulse-Arrival time estimation

The physiological definitions of PAT, PEP and PTT extrapolated to available signals in the study – Electrocardiogram, Impedance cardiogram and Photoplethysmogram – are described in figure 7. PAT is then obtained from markers in ECG and PPG.

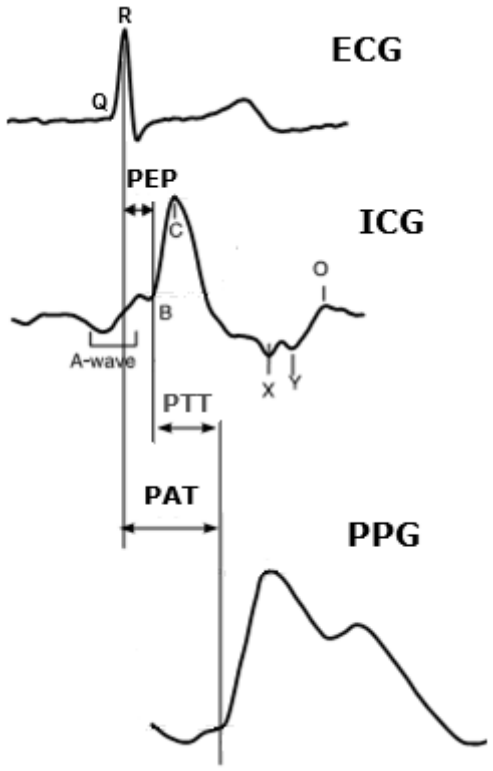

Figure 7 – Obtaining pulse arrival time, pulse transit time and pre-ejection period.

Pulse Arrival Time (**PAT**) = Pulse Transit Time (**PTT**) + Pre-ejection Period (**PEP**)

1. **QRS complex of the ECG** marks the beginning of contraction. The **R peak** is used as an alternative to Q wave as it is much easier and accurate to detect and the time between them, which is around 30 milliseconds, does not suffer significant variations. R peak detection is performed using a Pan-Tompkins [35] derived algorithm. Heart Rate in beats per minute is also attained from the inverse of intervals in minutes between R peaks (R-R interval).

2. **B point of the ICG** gives the moment of opening of the Aortic valve which determines the beginning of ejection of blood and the start of the pulse wave. There are alternatives in the methodology of observing this instant and PEP estimation, such as using heart sounds [36] and echocardiography.

3. **Foot/Onset PPG** gives the arrival of the pulse wave at the extremity. There are different PAT definitions applied throughout the literature using different marker points of the PGG signal. In this study the point of arrival of the pulse wave is determined, and it is calculated through the derivatives of the signal. Other markers can be used such as the peak of the wave (end of systolic period) or middle of systolic rise. There is also the possibility of

defining pulse arrival by backtracking from the middle of systolic rise, using its slope, to a diastolic level (a different option for foot of wave).

Beat-to-beat PAT: R peak of ECG to foot of corresponding PPG wave.

3.4. Pulse-Transit time estimation

3.4.1. True Pulse Transit Time

True Pulse Transit Time (PTT) is simply obtained by subtracting the available PEP from the estimated PAT. Two examples of obtained PAT, PEP and PTT signals are shown in Figure 8.

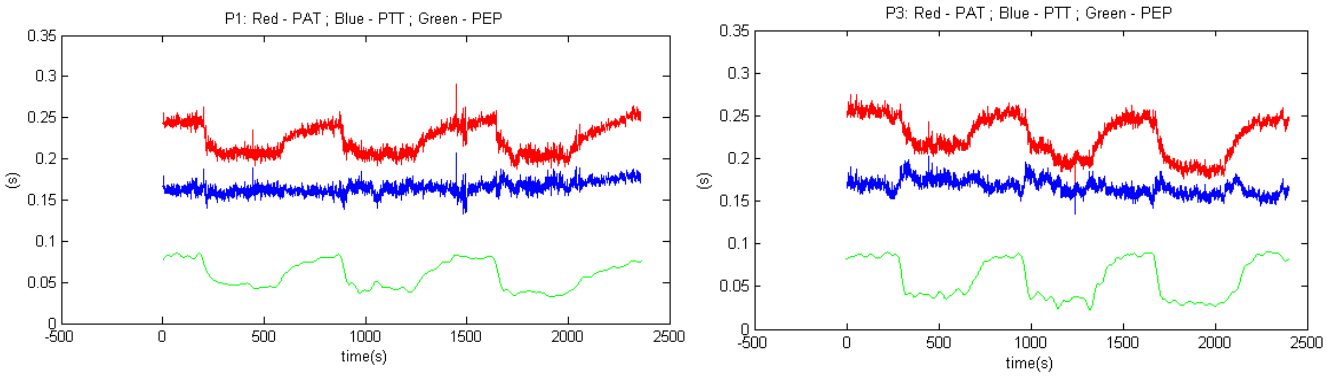

Figure 8 – Typical Results (two patients) of PTT (blue), PAT (Red) and PEP (green)

PTT would then infer over the propagation of the pulse wave in the arterial vessels starting on the aortic valve/proximal-aorta and ending in the finger (Fig. 9). It is inversely related to a mean pulse wave velocity through that segment. Even if the arteries along the pathway exhibit different behaviors, e.g., a less elastic radial artery, changes in pulse wave velocity in just a section of the path would inflict alterations in mean PWV and PTT.

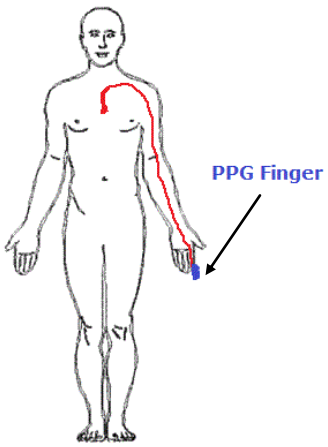

Figure 9 – Photoplethysmograph (PPG) setup, placed on a finger. The considered pulse transit time is related to the propagation of the pulse wave starting in the aortic valve until its arrival at the extremity (finger)

3.4.2. Difference of PTT

By using an extra PPG signal in an extremity closer to the heart, in this case the earlobe, two distinct pulse arrival moments for every single heartbeat are extracted and their difference in time estimated, thus getting a difference of PTT (DPTT) as portrayed in figure 10. The pulse wave is detectable first at the earlobe and later at the finger and the difference of their arrival time is not affected by PEP.

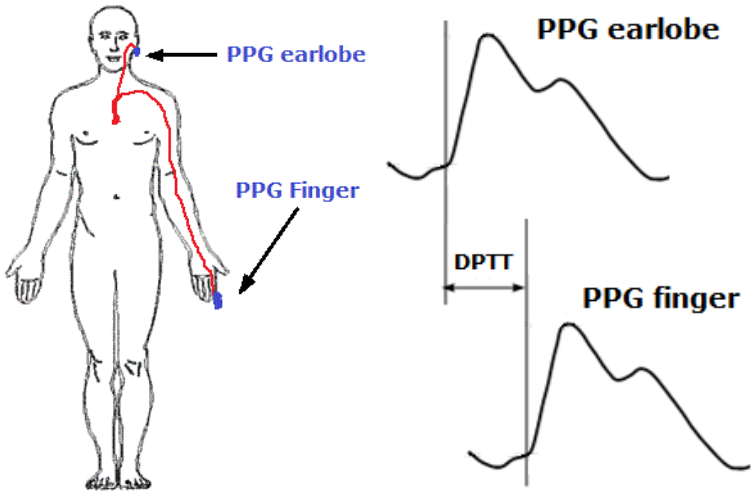

Figure 10 – Obtaining difference of PTTs (DPTT). PPG collocation (left) and estimation from signals (right)

4. Methodology of Pulse-Transit Time

4.1. The Moens-Korteweg equation

Pulse transit time and pulse wave velocity should be related to different aspects of the vessels in which the pulse wave propagates, and the blood that is flowing through them. Blood flow in an elastic artery is described mathematically through non-linear equations that state the motions of fluid and vessel wall, coupled equations based in the nature of fluid viscosity and interactions of the wall. Introducing simplifications can achieve a simpler and analytical solution which may lose some validity depending on the case study. The Moens-Korteweg equation (Equation 4.1) is such a solution, and a popular one, where it assumes that the rate of propagation of pressure waves in an elastic vessel is obtained from simple geometric and elastic properties of vessel wall:

$$PWV = \frac{\text{distance}}{PTT} = \sqrt{\frac{E\,h}{\rho 2 r_0}}, \tag{4.1}$$

Where E is the elasticity modulus of the vessel wall, h is its thickness, ρ is the density of blood, and r_0 is the radius of the vessel [37]. Backtracking to how this equation is derived provides additional insight on what is taken into account and the existent underlying assumptions, which should be important to analyze the questionability of results. This derivation of the Moens-Korteweg equation is executed in Annex 7.1.1. The main aspects of equation origin are the assumption of a non-viscous fluid and neglection of an area gradient in the mass conservation equation which will be important later on.

4.2. Blood pressure calibration

The Moens-Korteweg equation provides a connection between PWV and elasticity modulus, making it an attractive indicator of the elastic properties of the vessel wall, such as arterial stiffness. Higher stiffness indicates higher elasticity modulus and therefore higher PWV. Relating to blood pressure, the Hughes equation [38] has been derived by observing that the elastic modulus increases exponentially with the increase of blood pressure:

$$E = E_0 e^{\alpha P} \tag{4.2}$$

where $\alpha \approx 0.017\ mmHg^{-1}$. Pressure P in this case relates to a measure of the Mean Arterial Pressure (MAP). E_0 should be regarded as a reference elasticity state and depends on individual factors specific to a subject. Moreover, the parameters involved in the equations 4.1 and 4.2 are very subject-dependent and not easily measurable. To achieve a feasible connection of PTT and BP through calibration functions one has to further simplify by considering constant vessel thickness and radius which the M-K derivation already took into account, to a certain

extent. Subject-specific calibration can then be reached based on equations 4.1 and 4.2, in form of a logarithmic dependency by:

$$P = A\ln PTT + B \tag{4.3}$$

This would give a rough relationship of the two variables directly applicable on the true PTT estimation from single PPG setup. It should be emphasized that blood pressure is actually regulated by additional factors such as cardiac output, contractility, peripheral resistance and cardiac preload, and it is expected to at least observe an effect on PTT of some of these factors, especially peripheral resistance.

For the difference of PTTs (DPTT) from the double PPG setup it is not possible to directly apply the same equations without some analysis. This measure is not a PTT for a single vessel as it is assumed for the M-K model, since two arterial pathways – one to the ear *e* and the other to the finger *f* – are involved. There are two PTTs where $DPTT=PTT_f - PTT_e$ with arterial pathways of distance L_f and L_e:

$$DPTT = \frac{L_f}{PWV_f} - \frac{L_e}{PWV_e} \tag{4.4}$$

If we roughly assume the same mean PWV in both arterial branches and apply the M-K equation (Equation 4.1), this gives a DPTT of:

$$DPTT = \frac{L_f - L_e}{PWV} = \left(L_f - L_e\right)\sqrt{\frac{\rho 2r}{Eh}} \tag{4.5}$$

This equation has the same structure as equation 4.1 and the calibration function stated in equation 4.3 can be applied in the same fashion since the length of arterial pathways is constant and will simply enter in calibration parameters.

4.3. Model-based sensitivity

From the Moens-Korteweg based BP models, with the assumption of vessel radius and wall thickness remaining constant, an equation that relates theoretical changes in PTT to changes in blood pressure can be derived (complete derivation in Annex 7.1.2), i.e.

$$\Delta PTT = PTT0\left(\sqrt{e^{-\alpha\Delta P}} - 1\right) \tag{4.6}$$

where PTT_0 is the starting PTT, known for a given pressure P_0. The concept of pressure here still applies to mean arterial pressure. With $\alpha \approx 0.017\, mmHg^{-1}$ it is then possible to get a feeling of the magnitude of expected variations, considering three base PTTs (100, 150 and 200 ms) and a BP increase between 0 and 20 (fig. 11).

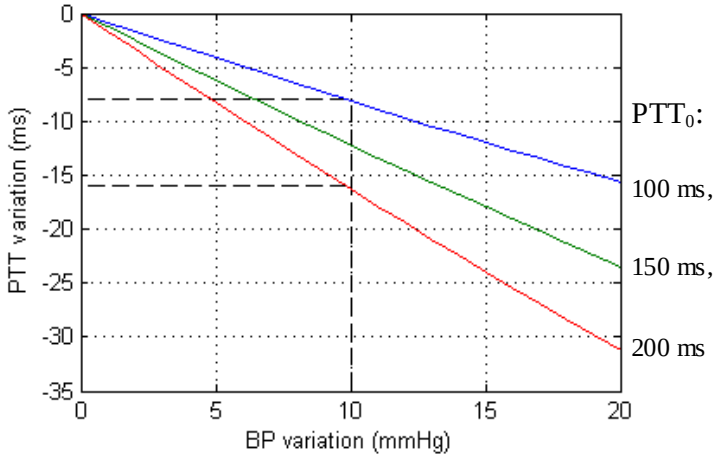

Figure 11 – Expected PTT variations for variations of Blood Pressure according to Moens-Kortweg and Hughes equations, with 3 different initial PTT values (PTT_0)

Using the model, it is determined that for a change in pressure, e.g., of 10 mmHg, with PTT0 in range of 100ms to 200ms, the order of magnitude of expected PTT variations is expected to be of about 8-16ms. Even though this estimation depends strongly on alpha parameter and ignores other vascular changes such as change in vessel radius, one can still take this approximated expected change into account for discussing the accuracy of the employed methods.

4.4. Accuracy of measurements

True PTT is obtained from the subtraction of PEP from PAT ($PTT = PAT - PEP$) and the uncertainty of a PTT measurement accumulates the uncertainties (σ) in both PAT and PEP estimation. Through error propagation and with function f for PTT:

$$f(PEP, PAT) \equiv PAT - PEP$$

$$\sigma_f^2 = \underbrace{\left(\frac{\partial f}{\partial PEP}\left(E(PEP), E(PAT)\right)\right)^2}_{=1} \sigma_{PEP}^2 + \underbrace{\left(\frac{\partial f}{\partial PAT}\left(E(PEP), E(PAT)\right)\right)^2}_{=1} \sigma_{PAT}^2 \quad (4.7)$$

PAT measurement error is determined by the accuracy in detecting the R-peak in the ECG and the systolic foot point of the PPG. R peak detection is fairly robust, with an estimated uncertainty of about half of the sampling time (5.0 ms), hence 2.5 ms. To determine the accuracy of detection of onset of the PPG systolic wave, a manual annotation of 50 heart beats was performed, by comparing the predicted foot points from the existing tool to where the onsets visually seem to be. This provided an uncertainty of 4 ± 8 milliseconds. This is not a definite accuracy, as there are other unquantified uncertainties related to where the onset should really be in the PPG as discussed in the previous chapter.

As for PEP measurements, the accuracy of values provided from the Niccomo device involving B point detection has been investigated in [39] using echocardiography as reference and was estimated to be 9.8 ± 21.4 ms. The use of echocardiography is not intended in our

setup. Heart sounds should also provide more accurate results as seen in [45] but it also imposes a change of setup.

From equation 4.7 and similarly for DPTT as difference of PPG foot points, uncertainties of both PTT and DPTT can be estimated:

$\delta PTT \approx \pm 23$ ms

$\delta DPTT \approx \pm 11$ ms.

The accuracy of the blood pressure references, given from the Portapres device is also investigated. There is a discrepancy when comparing it with a cuff-based measurement, performed intermittently (figure 12).

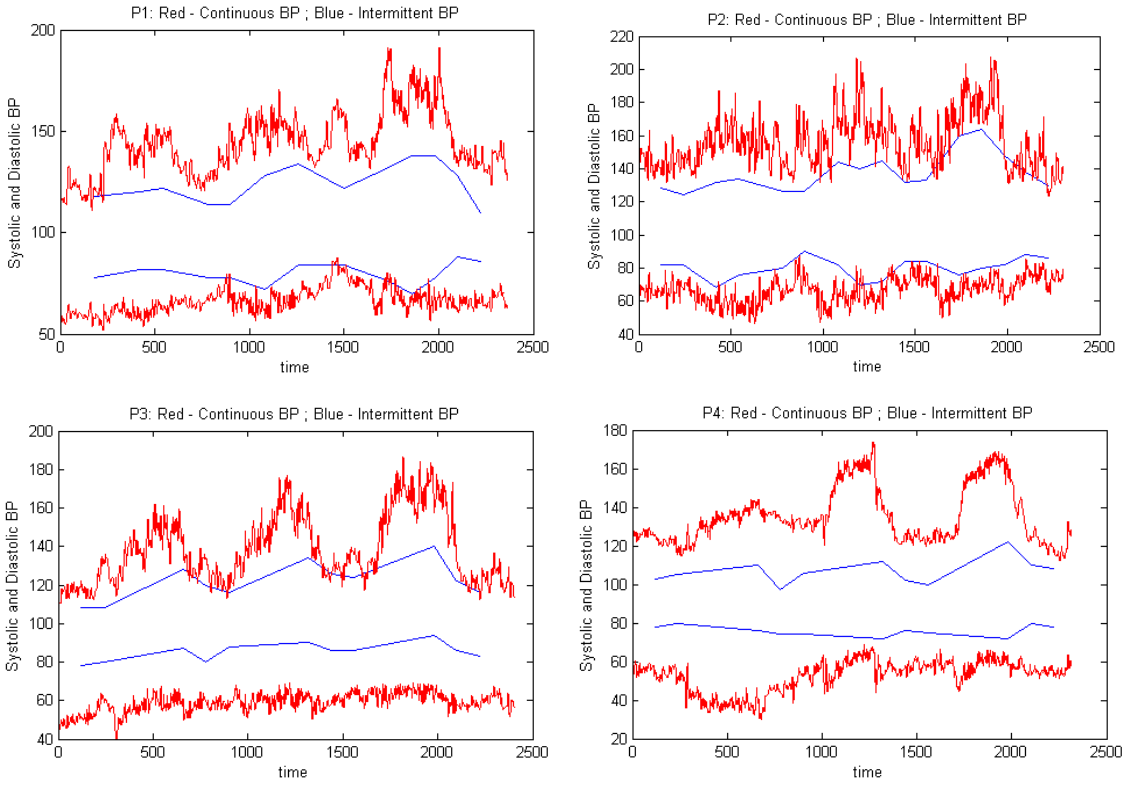

Figure 12 – Systolic (higher) and Diastolic (lower) values of Blood Pressure (mmHg) given by the Portapres device (red) and by intermittent cuff-based method (blue).

We can observe that Diastolic values from the Portapres are usually lower than given by the cuff-based method, and Systolic values are higher. Note that the Portapres device has regular calibration measurements, using an inflatable cuff. Differences of continuous and intermittent BP are up to 30 mmHg and despite the intermittent values not being very frequent, pressure variations seem to be followed. Therefore, it can be stated that the values from Portapres should not be treated as invalid, and if they demonstrate the 'real' behavior of blood pressure changes, available signals are good enough for the intended calibration purposes.

4.5. Results

4.5.1. Typical Measurements and signals

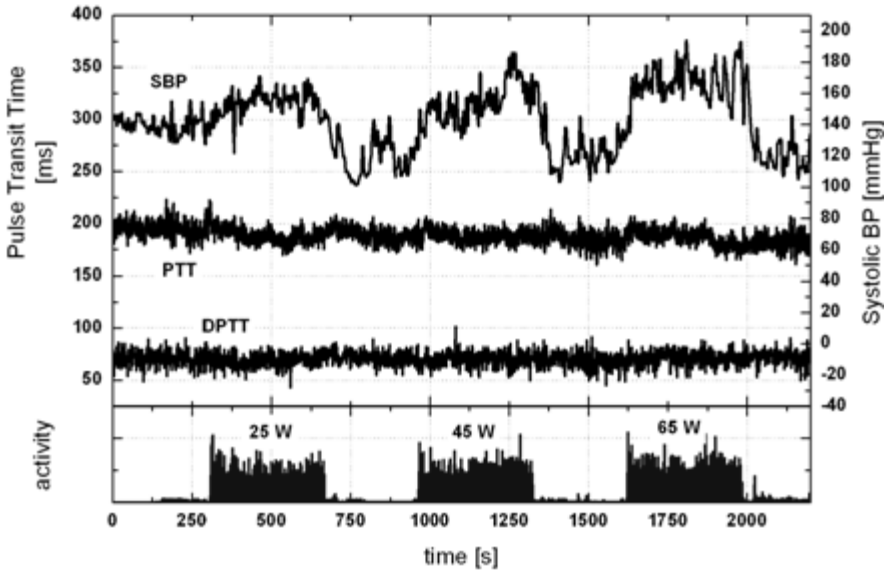

Figure 13 – Pulse transit time to fingertip (PTT), difference of PTT from finger and earlobe (DPTT) and systolic blood pressure (SBP) for complete sequence for one subject. Physical activity periods are also shown. Typically no specific change in PTTs or DPTT could be observed.

Figure 13 depicts an example set of signals of SBP, PTT, DPTT and activity level for a complete measurement sequence for one subject. As illustrated, when the subject was at rest at the beginning of the test, SBP was about 140 mmHg, PTT was about 200 ms and DPTT about 70 ms.

Diastolic Blood Pressure does not seem to exhibit significant changes for our short physical effort runs contrarily to Systolic Blood Pressure which pronouncedly rises during exercise periods, and therefore seemed to be the most predictable. As a consequence, Mean Arterial Pressure follows a similar trend to SBP, though variations are shorter, as seen in figure 14. With this, it is decided to avoid the use of DBP, needed to calculate MAP, and thus SBP is explored as the only pressure measure throughout this analysis, reliable and able to express the changes in mean pressure. By using SBP instead of MAP correlations should not be influenced and on calibration functions where MAP was implicit, values should change proportionally.

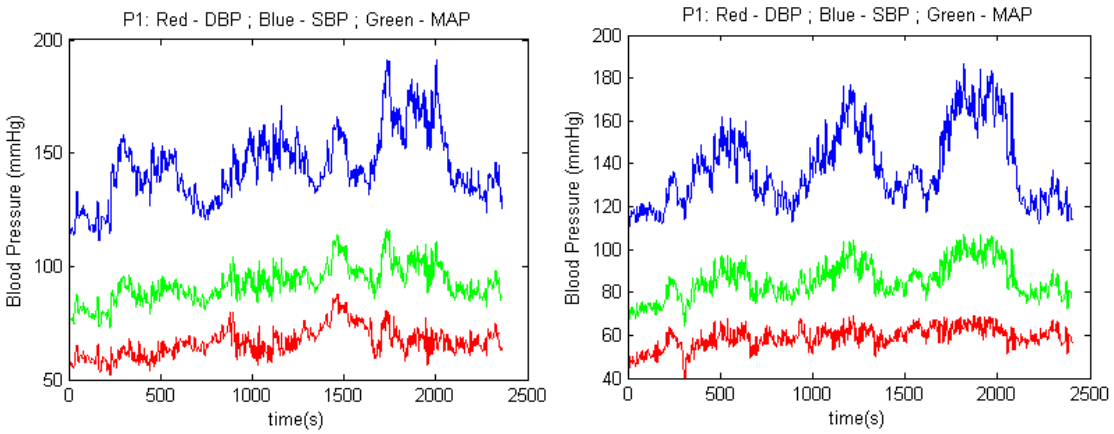

Figure 14 – Typical results of Diastolic (DBP) and Systolic Blood Pressure (SBP) and Mean Arterial Pressure (MAP).

Still from figure 13, PTT and DPTT neither show a response to SBP nor follow any specific trend, which was consistently observed throughout the test subjects. Consequently, it can already be foreseen that PTT measures will not correlate well to SBP.

In PTT as well as in DPTT there is a large and short-term signal variability that goes up to approximately 25 milliseconds. This large variance appears in PAT (and consequalty in PTT) and correlates well with breathing activity monitored with the respiration band as observable in figure 15. This effect of respiration has been described in [40].

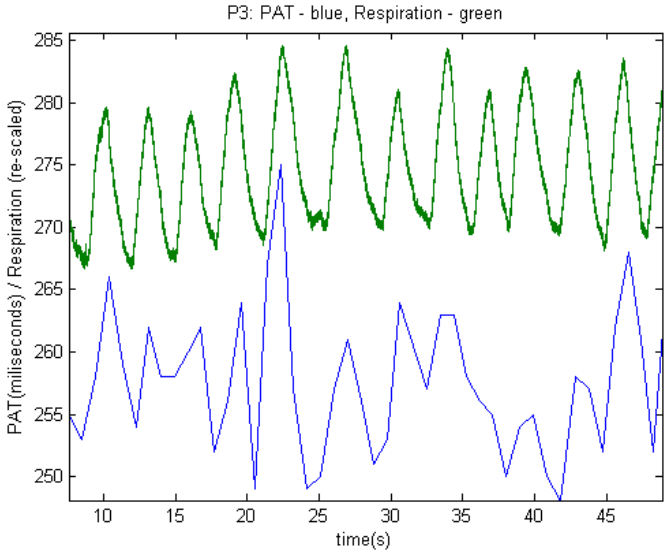

Figure 15 – Pulse Arrival time (blue) and Respiration (green, re-scaled) for a ~50 sec period at rest of one subject

It is observable that PAT is usually higher when inspiration occurs, although exact effect on values of PAT cannot be predicted. These PAT signals where kept when observing linear fitting, but for analysis of each exercise and recovery run, simple averaging/filtering was performed to easily observe variation trends.

4.5.2. Statistics, Correlation and Calibration

Summarized in table 1 are the average measurement effects for SBP, DBP, PEP, PTT and DPTT for the study population and the different power levels compared to their values at the beginning of the test. Complete table of related subject values is in annex 7.2.3. PTT and DPTT don't show any specific variation pattern.

	D_SBP (mmHg)	D_PAT (ms)	D_PEP (ms)	D_PTT (ms)	D_DPTT (ms)
25 W	30±13	-45±10	-46±10	1±9	3±4
45 W	39±20	-54±13	-52±11	-1±10	2±5
65 W	54±30	-60±15	-55±12	-3±11	1±5

Table 1 – Average exercise changes for SBP, DBP, PEP, PTT and DPTT (average ± standard deviation)

To evaluate the relationship between PTT/DPTT/PAT and SBP, linear correlation is employed. The straight linear correlation is analyzed as well as after the calibration transformation of equation 4.3 (being a logarithmical change, it is marked with and *ln* index). Complete statistics are in annex 7.2.4; a summary of average correlation results is presented in table 2.

Variable	Correlation with SBP (average ± standard deviation)
PTT	-0.19 ± 0.45
PTT_{ln}	0.22 ± 0.46
DPTT	0.22 ± 0.46
$DPTT_{ln}$	-0.22 ± 0.45
PAT	-0.84 ± 0.09
PAT_{ln}	0.85 ± 0.09

Table 2 – Average correlation results for PTT, DPTT and PAT and for the corresponding calibration logarithmic alteration (ln index)

Correlations for PTT and DPTT are generally low and inconclusive, with a high variability, being either positive or negative, whereas theoretically, we expected negative correlation for PTT and positive correlation after a logarithmic transformation. Examples of PTT vs. SBP plots for linear fits are depicted in figure 16. Dispersed data point clouds result of such depiction, and the results of low correlation of PTTs are clear.

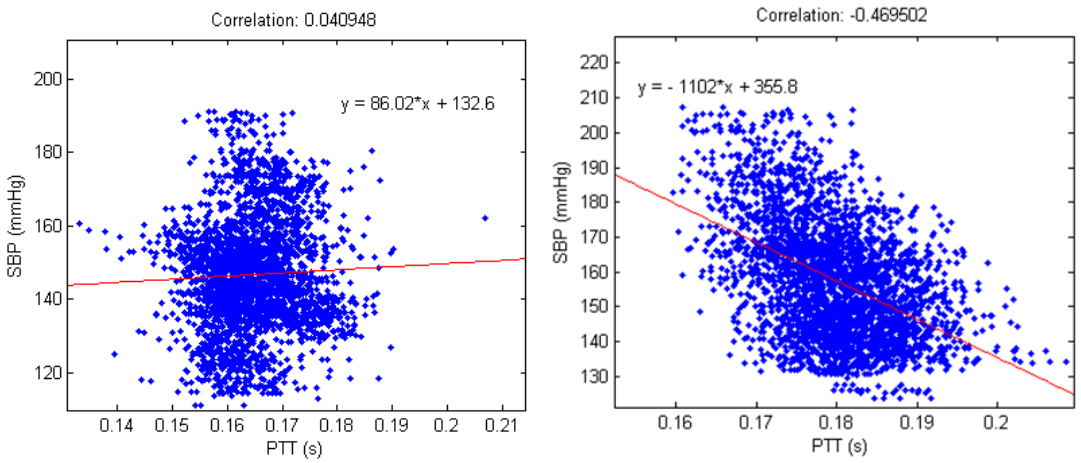

Figure 16 – Typical results of systolic blood pressure in order of pulse transit time for 2 subjects, with linear fit

On the other hand, for PAT and PAT_{ln}, a high correlation with SBP is observed, but with the logarithmical transformation only showing a marginal improved correlation.

Based on the calibration function 4.3 the free coefficients *A* and *B* have been determined, with a summary on table 3 (complete table in annex 7.2.5), and *A* is an indicator of the sensitivity of a particular measure to SBP. For PTTln and $DPTT_{ln}$ no consistent values for *A* could be obtained as it was expected from the previous analyses, whereas for PAT_{ln} *A* is negative, however with a large subject-specific variance.

Variable	A (average ± standard deviation [min. – max.])	B (average ± standard deviation)
PTT	-92 ± 187 [-398 – 234]	-29 ± 333
DPTT	-26± 157 [-421 – 224]	217 ± 501
PAT	-178 ± 57 [-294 – -124]	52 ± 31

Table 3 – Average results of parameters A and B of the SBP calibration equation applied for PTT, DPTT and PAT

4.6. Discussion

The obtained results suggest that PTT and DPTT are not good measures to monitor physical exercise induced BP changes in a young, healthy population. The limited measurement accuracies of the used setups may be one of the reasons why. Specifically, the measurement accuracy to extract PEP based on the ICG (9.8 ± 21.37 ms) seems too large if one had theoretical expected 8-16ms PTT changes for a 10mmHg BP change. Plotting PTT variation against SBP variation together with theoretical values from the sensitivity model (equation 4.6) including deviations due to measurement uncertainties as in figure 17, it is observed that between the standard deviation lines, a very significant part of the obtained PTT and SBP pairs is covered. Therefore, this points to the fact that if there are any small PTT variations due to exercise, the used setup may not have the necessary sensitivity for correctly detecting them.

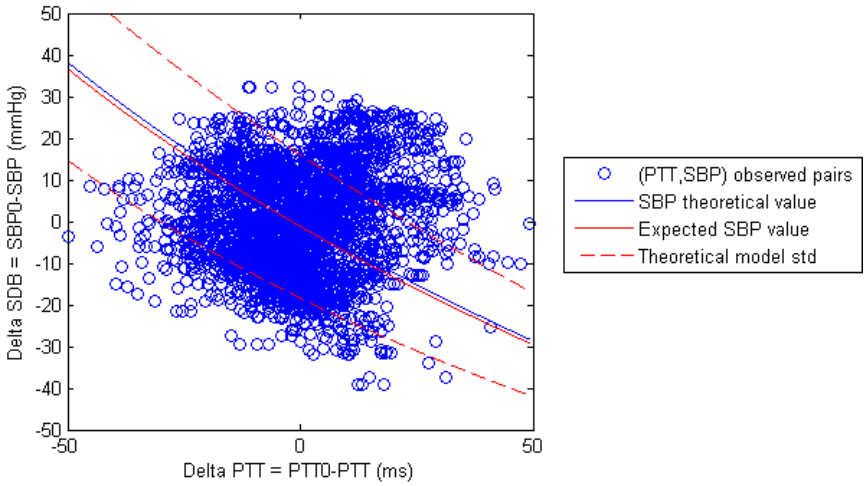

Figure 17 – Finger Pulse transit time (PTT) variations with systolic blood pressure (SBP) variations for the entire study run in one subject, including theoretical expected variations and standard deviations from measurement uncertainties.

With the alternative PTT method (DPTT), using two PPG at fingertip and earlobe and getting a PEP-free estimation not corrupted by PEP estimation errors, the measured DPTT also did not show a consistent correlation with exercise induced SBP variations. Even if in this case the measurement accuracy is much better, there might be other uncertainties that can make DPTT an unreliable indicator of true PTT or SBP. These might come due to the two pulse propagation properties in the two distinct arterial pathways.

The validity of applying the Moens-Korteweg (M-K) equation (4.1) should also be analyzed. The equation has been derived from a simplified mechanical model assuming that there are insignificant variations of vessel radius and section, as shown by the previously mentioned area gradient that was dropped. This may not be true for large arteries as considered in [41,42,43], especially for healthy young subjects. This population is normally characterized by elastic and compliant arteries, where a blood pressure increase would be accompanied by a larger radius at the passage of the pressure pulse. However, such effects are not taken into account in M-K. Taking pressure dependent changes in radius into account, we can estimate a

new sensitivity as in equation 4.6, with $\Delta R/R=0.002$ /mmHg in the ascending aorta [44]. This results in expected PTT changes of 5-11ms for a 10 mmHg mean pressure change, representing a 33% decrease compared with the previous change of 8-16ms. Therefore, considering radius variations should help in obtaining BP, but measuring them would not be adequately practical in the unsophisticated, continuous and non-invasive monitoring application this study addresses. On the other hand, for stiff arteries typical of older subjects, radius variations would not be as significant and probably larger effects on PWV/PTT could be observed.

PAT provided consistent correlation results as was observed before in a similar exercise scenario [25]. High correlation for such experimental settings is mainly due to the prominence of PEP whose effects are not covered by the M-K model at all.

5. *Heart Rate and Pulse-Arrival Time in physical exercise*

With PTT not exhibiting any attractive variations in the physical exercise data, it was aimed to investigate the signals that always seem to display, to a certain extent, similar and strict variation patterns throughout the study subjects. These were heart rate and pulse arrival time and their variation details were studied and attempted to model. Initially presented are the modeling attempts for each of them separately.

5.1. Heart Rate variation

5.1.1. HR model

Hájek et al. [45] proposed a model of heart rate regulation and response in physical exercise which becomes simple enough for implementation in this work and easy determinability of model parameters. It constitutes a straightforward representation of mechanisms involved in regulating the increasing heart rate responding to physical effort, more precisely, describing a fast action due to vagal inhibition (inhibiting parasympathetic activity) and a slower acting neurohormonal component due to complex control from the sympathetic system. The block diagram of this model is shown in figure 18 and its structure is as follows:

y – the output, being the Heart Rate variation in Hz.

$\mathbf{x_1}$ – the feed-forward and rapid component of nervous origin;

$\mathbf{x_2}$ – the slow neurohormonal component with feedback.

The inputs:

$\mathbf{u_1}$ – takes the value of 0 if no exercise is in effect (rest and recovery) and the value of 1 when exercising;

$\mathbf{u_2}$ – the exercise load values in watts (W). If no load is being applied, value is 0.

To characterize both components x_1 and x_2 there is a pair of time constants and gains, consisting in the 4 parameters that describe the entire system: $\mathbf{K_1}$, $\mathbf{T_1}$, $\mathbf{K_{ref}}$ and $\mathbf{T_i}$.

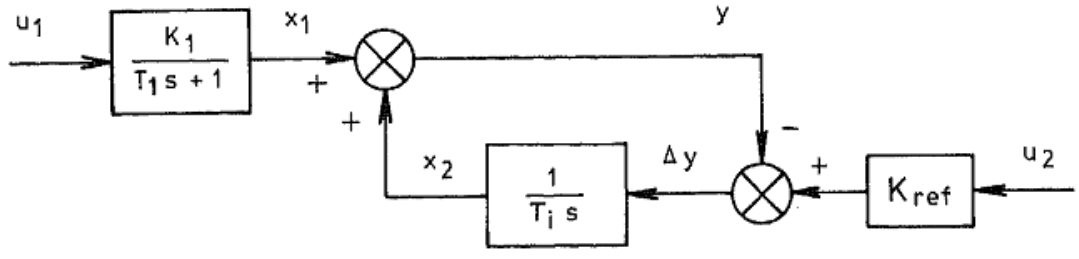

Figure 18 – Block diagram of the heart rate regulation system, adapted from [45].

Replicating this model in Matlab's Simulink, it was possible to reproduce a similar result (figure 19) to the exemplified on the paper for volunteer no.2, with an increasing exercise load, a slope from 0 to 196.2 W, spanning 4 minutes.

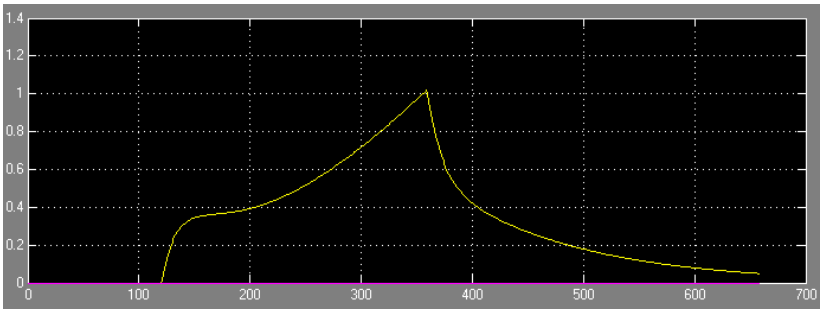

Figure 19 – Heart rate variation response as replicated from [45].

HR is here in Hz as in the paper and a change of HR is obtained (the ~1 Hz peak would correspond to ~60 Beats per minute (BPM) HR change). Notice the initial fast response from parasympathetic inhibition and another long lasting effect always coping with the increasing exercise load. There is no direct dependency to the initial HR state although a relation can probably be imbued in different parameter values. Even if this means that, for the same subject, different initial HR would lead to a different response and model parameters, the HR level at rest should already be and indicative of cardiovascular condition.

Figure 20 illustrates the HR response in BPM using the same parameters from the previous example for the three times repeated 6 minute exercise 5 minute recovery setup with 25W, 45W and 65W workload, similar to what is performed in our dataset.

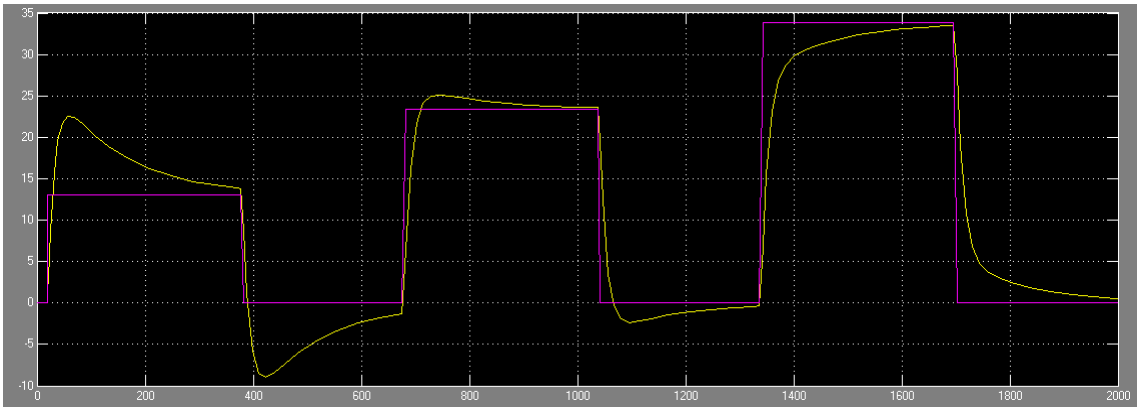

Figure 20 – Simulation of 25/45/65W exercise using model and parameters from [45];
Yellow line – output HR; Purple Line – Kref * Load

For 25W, a great overshoot is observed. Maximum HR is achieved in approximately 1 minute and then steadily decreases to a set level. The overshoot is observed occasionally in our datasets as exemplified in figure 21, although it is not as large.

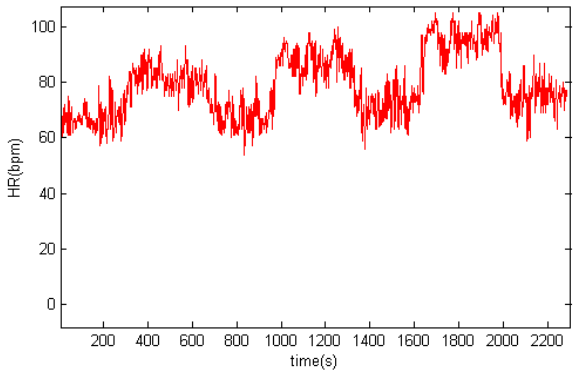

Figure 21 – Example of heart rate signal for subject X. A small overshoot of HR in first exercise can be observed.

Before trying to estimate the parameters for our data, it is necessary to carefully comprehend the effect of changes in the parameters of the model and their importance in a physiological point of view:

K_{ref} (Hz/W) – defined as a Heart Rate increment related to the load of 1 W. By multiplying K_{ref} and the exercise load, it defines the HR change level that the model has a tendency to settle in the final stage of each exercise run, as seen through the purple lines in figure 20. Therefore, it is responsible for final HR variation.

K_1/K_{ref} (W) – K_1 (Hz) is the gain from the first component x_1 and this ratio K_1/K_{ref} represents the load which can be coped with by this fast acting feed-forward component. The effects of different K_1 values are shown in figure 22. Normally, if **K_1/K_{ref} << Exercise Load**, there is an extra posterior effort during exercise with an increasing HR. Otherwise, overshoot occurs.

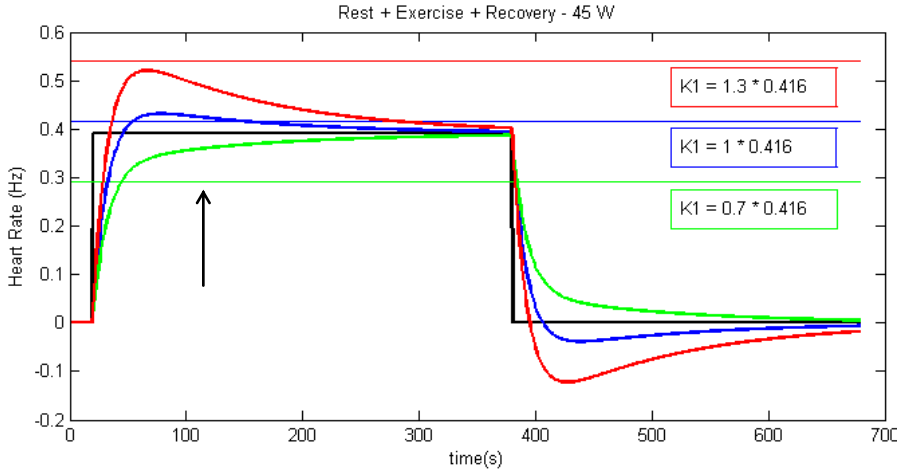

Figure 22 – Effect of increasing K_1 in a 45 W exercise. K_1/K_{ref} is 34W(green), 48W(blue) and 62W(red)

T_1 (s) – time constant of the feed-forward component. As seen in figure 23, T_1 mainly defines the initial HR change slope.

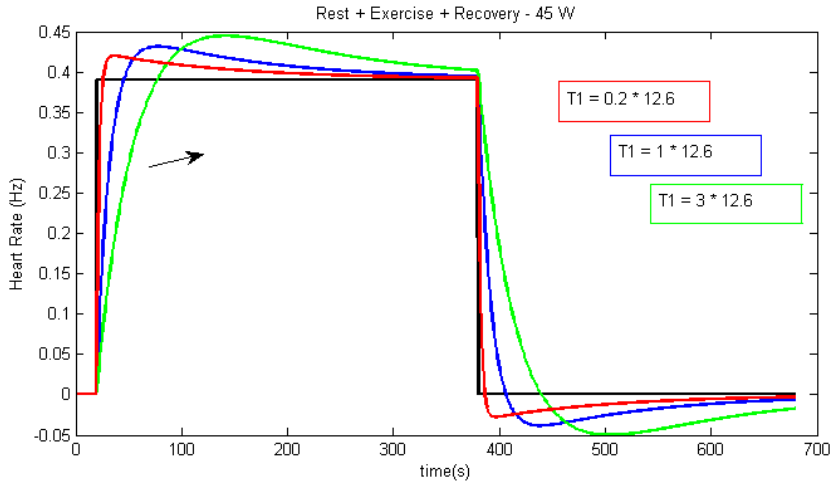

Figure 23 – Effect of increasing T_1 in a 45 W exercise. T_1 is 2.52s (red), 12.6s (blue) and 37.8s (green)

T_i (s) – time constant of the feed-back component. It is responsible for the rate in which the final HR level is reached, due to the long duration action (figure 24).

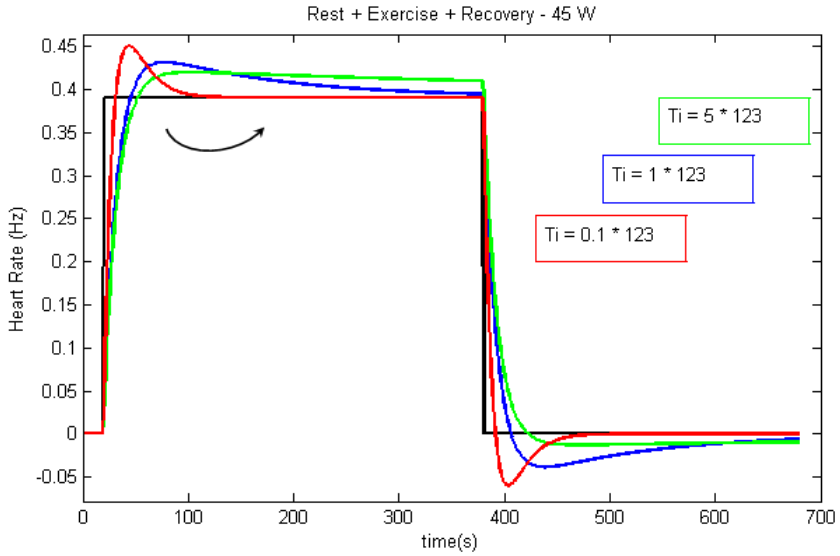

Figure 24 – Effect of increasing T_i in a 45 W exercise. T_i is 12s (red), 123s (blue) and 615s (green)

5.1.2. Parameter estimation through system identification

The next step was to try to estimate parameter values for sets of the data. Using the same state-space model of the paper, one can identify the system through the System Identification (SI) toolbox in Matlab. From the considered system:

State-space model: $dx/dt = A\,x(t) + B\,u(t) + K\,e(t)$

$y(t) = C\,x(t) + D\,u(t) + e(t)$

Which gives, neglecting errors:

$$\begin{bmatrix} \dot{x}_1 \\ \dot{x}_2 \end{bmatrix} = \begin{bmatrix} -\frac{1}{T_1} & 0 \\ -\frac{1}{T_i} & -\frac{1}{T_i} \end{bmatrix} \begin{bmatrix} x_1 \\ x_2 \end{bmatrix} + \begin{bmatrix} \frac{K_1}{T_1} & 0 \\ 0 & \frac{K_{ref}}{T_i} \end{bmatrix} \begin{bmatrix} u_1 \\ u_2 \end{bmatrix} \quad (5.1)$$

$$y = \begin{bmatrix} 1 & 1 \end{bmatrix} \begin{bmatrix} x_1 \\ x_2 \end{bmatrix} \quad (5.2)$$

These matrixes can be defined using the SI toolbox, and be identified automatically using a minimal error approach. To see how well the identification process behaves I provide the original model output and try to identify the parameters; the fit of the obtained result is in figure 25.

Original paper parameters:

T_1 = 12.6

T_i = 123

K_1 = 0.416

K_{ref} = 0.00868

Same setup as paper with 99,28 % fit (free parameter estimation):

T_1 = 11.8240

T_i = 121.0586

K_1 = 0.4120

K_{ref} = 0.0085

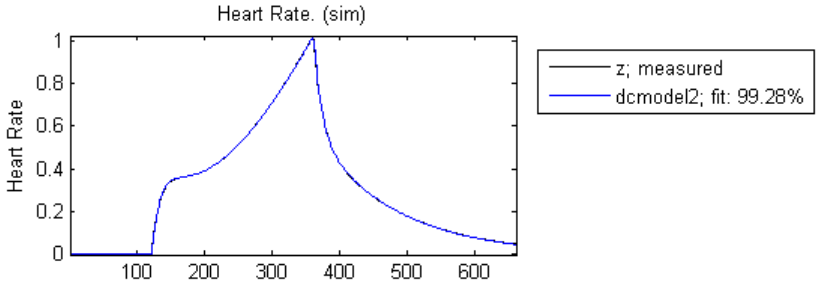

Figure 25 – Fit of identified model (dcmodel2) to original paper result

It is seen that the parameters are different by a small amount, although fit result is very high. To diminish variability of results it should be attempted to estimate and manually fix some variable, and the easiest to approach is K_{ref}.

From the K_{ref} definition, it is simple to estimate in our data of sequential exercise runs by dividing HR change at end of exercise by the corresponding exercise load. Figure 26 shows the obtained K_{ref}s in bpm/W for the 3 exercise levels for each subject.

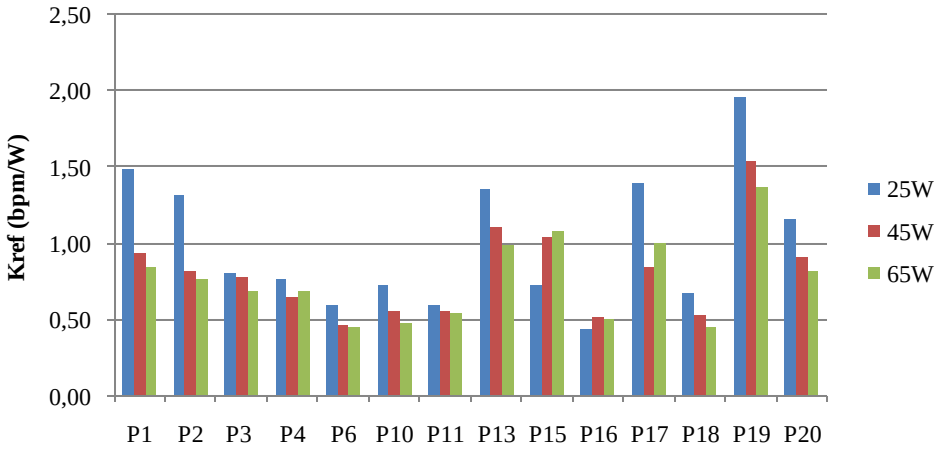

Figure 26 – Kref parameter for each subject in the 3 exercise runs. It is calculated by dividing end-stage exercise HR change (bpm) per Exercise Load (1 W)

	25W	45W	65W
MAX	1,96	1,53	1,37
MIN	0,44	0,47	0,45
AVG	1,00	0,80	0,76
STD	0,44	0,30	0,28

Table 4 – Average and deviation results for manually estimated K_{ref}

There are different behaviors of K_{ref} variability but the average result (Table 4) is that K_{ref} isn't always constant, and the HR change/Load response is larger for 25W. Still, this manually estimated K_{ref} would be implemented and fixed during automatic identification of other parameters.

Estimation is done until the end of exercise in each run. Figure 27 and figure 28 represent opposite cases of load which can be coped with the feed-forward component (K_1/K_{ref}). For subject 20 with 45W exercise, K_1/K_{ref} is 18.5W (much smaller than 45W load) and HR keeps increasing after initial response; for subject 16 with 25W exercise, K_1/K_{ref} is 42.5W (much larger than 25W load) and a big overshoot occurs.

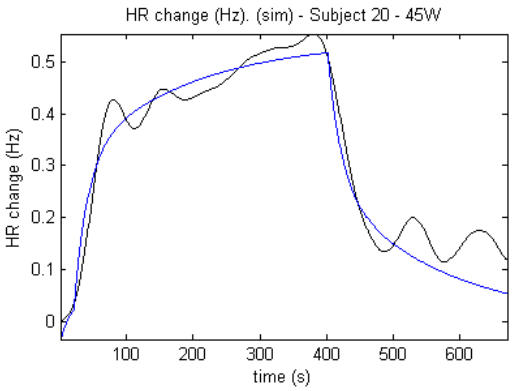

Figure 27 – Example of undershoot, identified for subject 20, 45W exercise. K_1/K_{ref} = 18.5W

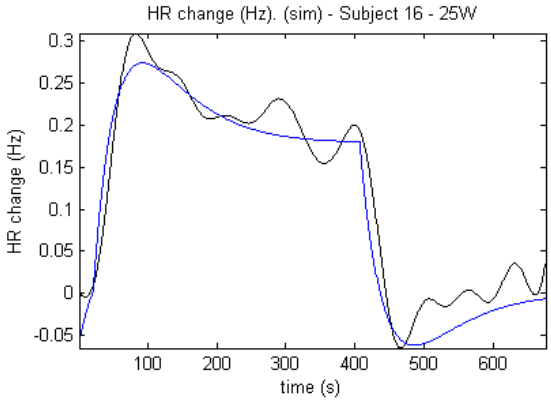

Figure 28 – Example of overshoot, identified for subject 16, 25W exercise. K_1/K_{ref} = 42.5W

In figure 29 and table 5, the results of fits and parameters for system identification in subject 1 are presented. It is primarily noticeable that parameters change depending on the exercise run.

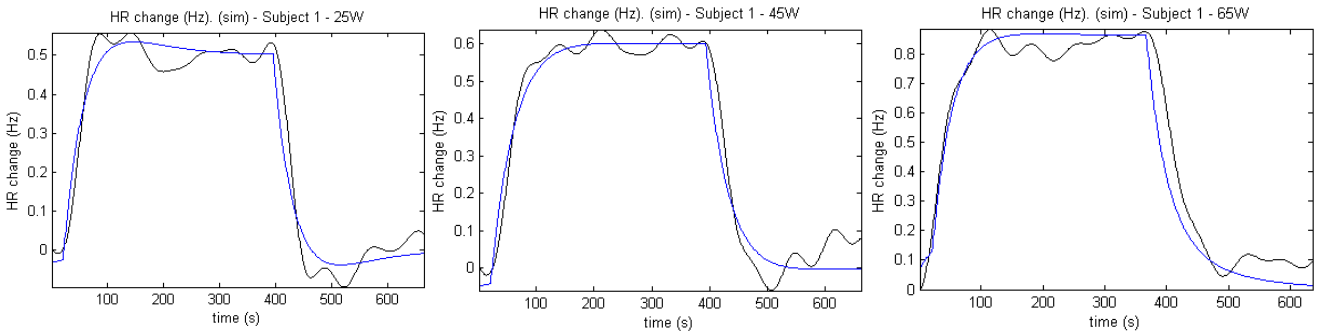

Figure 29 – HR model estimation fits for subject 1 in 25W, 45W and 65 W exercises.

Subject 1	25W	45W	65W
T1	52.263193	49.528051	32.414812
Ti	52.265506	51.155661	100.550461
K1	0.382699	0.208828	0.449542
Kref	0.020041	0.013347	0.013290
K1/Kref	**19.0959**	**15.6463**	**33.8251**

Table 5 – HR model estimated parameters for subject 1 for all exercise runs

5.1.3. Final model remarks

From figure 23 and 24, it is seen that T_1 and T_i can also influence, even if only slightly, the slopes corresponding to the other's direct action. Together with an adjustment of overshoot height from K_1, it is comprehensible that very different parameter combinations can be obtained for similar behaviors. Figure 30 demonstrates this fact where by employing different initial parameter guesses for identification (but fixing K_{ref} with the manually calculated value), different parameter results can be obtained with a very similar graphical outcome.

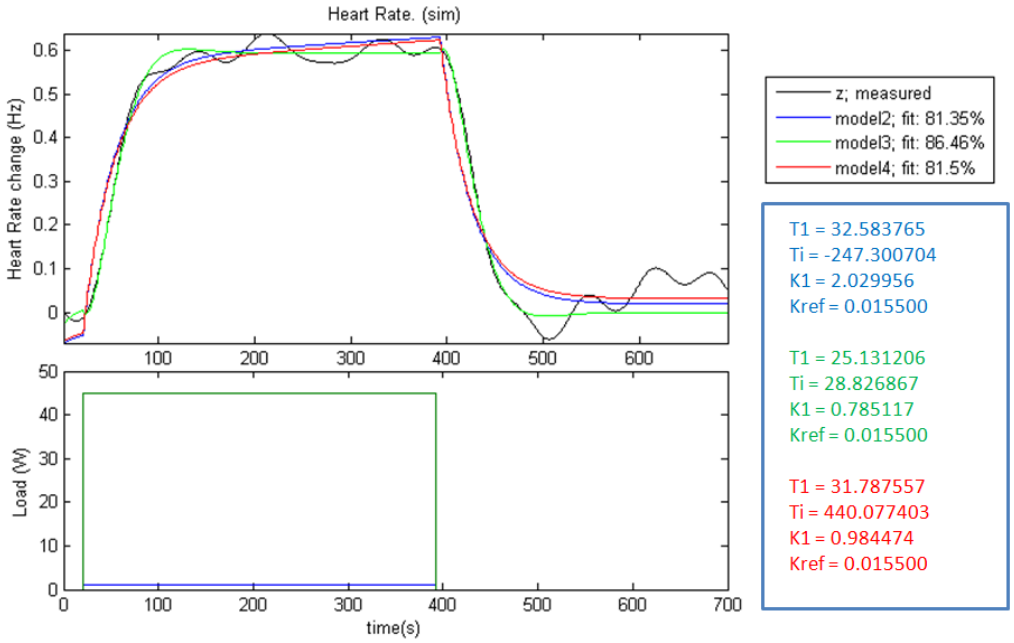

Figure 30 – Different results from identification for the same data piece. Manually fixed K_{ref}

The problem of result variability influences greatly what one can extrapolate out of this analysis and no other solution to this problem was found. The fact that some parameters are directly connected in the state-space model made it not possible to get any other valid form of parameter fixing or conditioning. There can also be the issue that using a 25 W (etc.) step (even if realistically the change of load is not instant) is very different than the paper setup of continuous increase in load.

5.2. *PAT variation*

5.2.1. Exponential fit

When an exercise run ends, PAT takes a long time to recover to a stable level. Modeling and comparing the characteristics of this variation is important for the final grasp of cardiovascular condition analysis. At first glance this variation of PAT seems to follow an exponential evolution (figure 31), prompting an investigation of fitting an exponential equation to this part (equation 5.3).

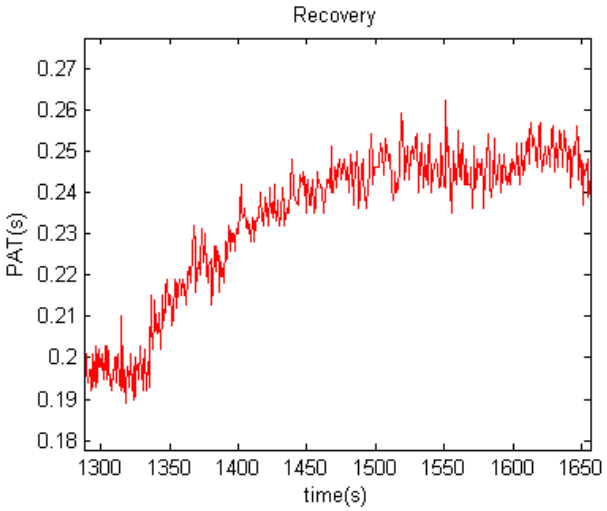

Figure 31 – Recovery of PAT after exercise, example from one subject.

$$PAT = A - Be^{-\frac{t}{\tau}} \tag{5.3}$$

A, *B* and τ ('tau') are the parameters for equation fitting: the level *A* sets the tendency of final PAT value, i.e., for an infinite time; *A* – *B* is the initial PAT level right after exercise; the most interesting parameter would be τ as it sets the width of the exponential variation, for constant values of A and B. Increasing τ implies a longer recovery of PAT as is depicted in figure 32.

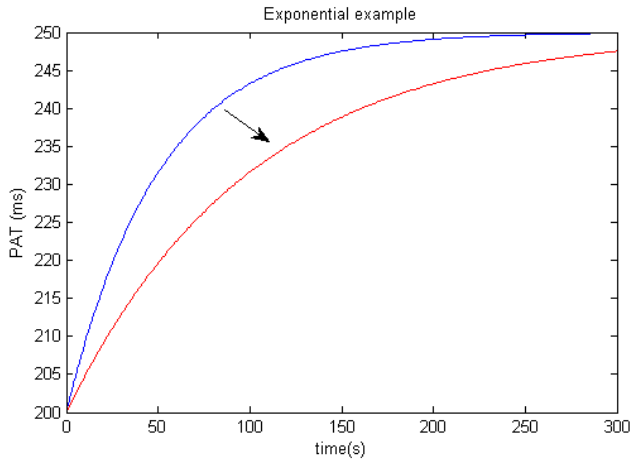

Figure 32 – Exponential and theoretical example for PAT recovery, with increasing Tau (blue=50 s, red=100s)

Moving to actual data, exponential fits were made in Matlab and it was necessary to choose the raw PAT signals or the low-pass filtered versions to execute the fits. Depicted in figure 33, raw signal contains the previously mentioned respiration effects and since filtered signal fits may slightly change, even though they are clearer, it is decided to use the raw and unfiltered versions.

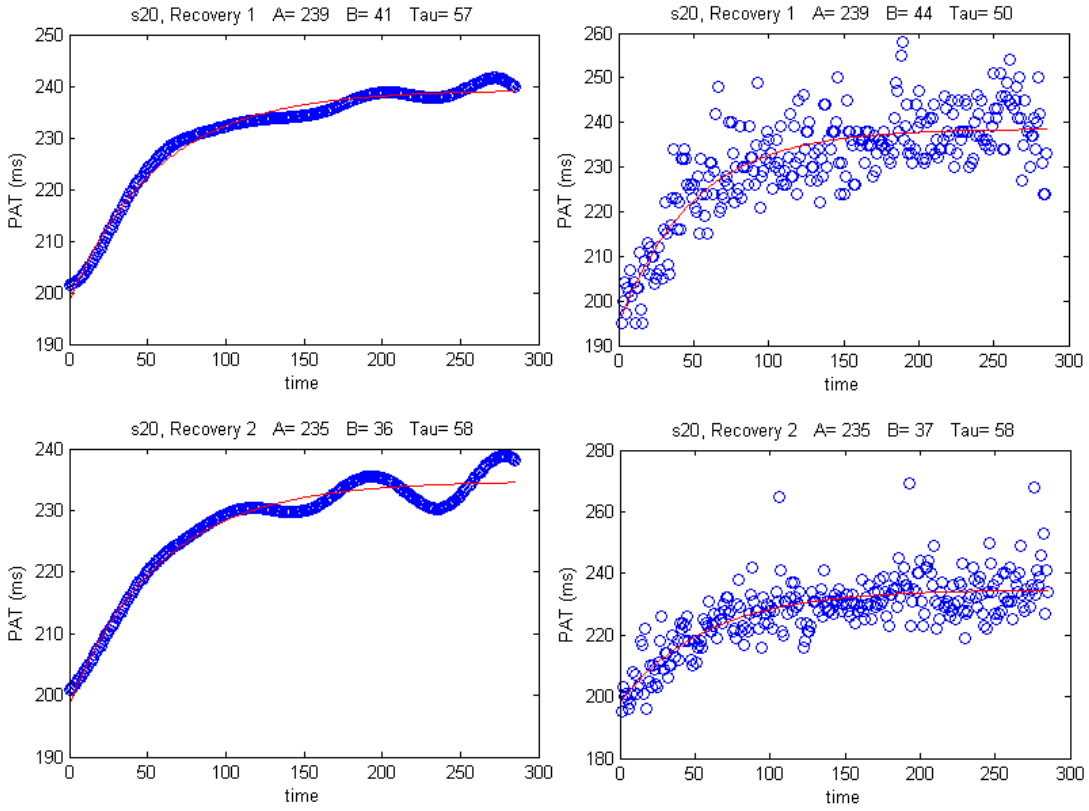

Figure 33 – Filtered and raw versions of 2 distinct PAT recovery periods in subject 20 with respective exponential fit and parameters.

Table 6 presents the average and standard deviation results for the exponential fits to our data (boxplots in annex 7.2.6). Delta A, B and τ represent the average of parameter increase for each patient, being the 45W percentage correspondent to the increase of parameter value from 25W to 45W exercise run, and the 65W percentage the increase from 45W to 65W. These average values are subsequently independent from the different absolute values among the group.

		A	B	τ	Delta A	Delta B	Delta τ
25W	AVG	257,66	47,61	93,43			
45W		257,97	56,67	109,07	0,02%	23,09%	26,26%
65W		263,59	65,23	137,13	2,09%	14,24%	29,40%
25W	STD	23,46	15,59	60,22			
45W		28,00	17,45	57,14	3,63%	36,51%	52,53%
65W		32,29	24,66	84,59	3,46%	16,50%	41,44%

Table 6 – averages for exponential fit parameters A, B and τ and relative variations from each exercise sequence

As expected, the baseline defined by A does not change significantly. On the other hand, B and τ parameters averagely grow bigger with increase in exercise load, although variance is very high. Some examples of τ evolution are depicted in figure 34, confirming that this evolution dependent on load is variable.

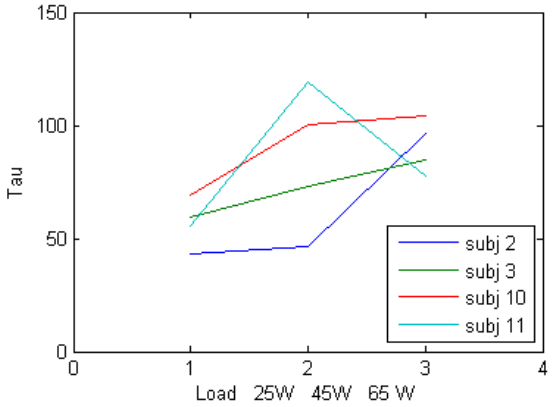

Figure 34 – Four subject examples of parameter τ evolution for 1/2/3=25/45/65W exercise load.

In figure 35, an example of exponential fit result for the 3 exercise loads is presented, along a 5 minute period such as the one of recovery setup. By reaching a time of 5 times τ in equation 5.3, value of PAT rises by 99% of *B* value, getting very close to the baseline defined by A and it can be said that PAT has stabilized.

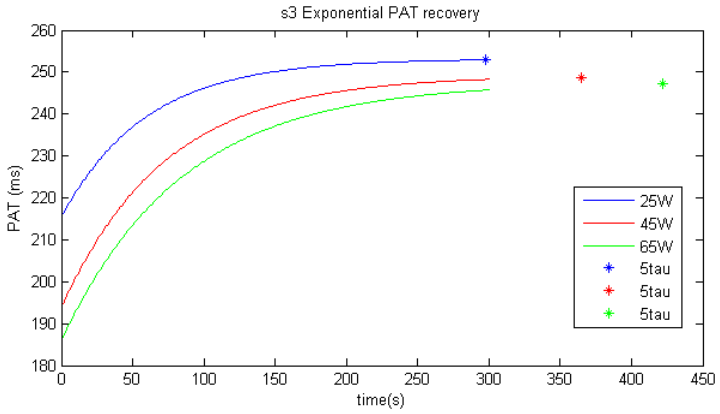

Figure 35 – Example of fits for PAT recovery of subject 3;
A is 253/249/248, B is 38/55/61 and τ is 60/73/84s for the 25/45/65W exercise load respectively.

The presented example corresponds to one of the lowest τ combinations in the data. The majority of subjects have the 5τ point outside the 5 minute period which means that PAT may not always recover in its entirety during the allowed time for recovery in the study.

The average parameter results (from table 6) are put in graphical form in figure 36. The simultaneous increase of B and τ provide similar initial PAT variation slopes for the different exercise loads (hinting for a limit of PAT recovery speed). Nevertheless it is expected that anomalous behaviors, such as a patient with a cardiovascular status that makes PAT recovery harder, be represented with a large increase in the τ constant.

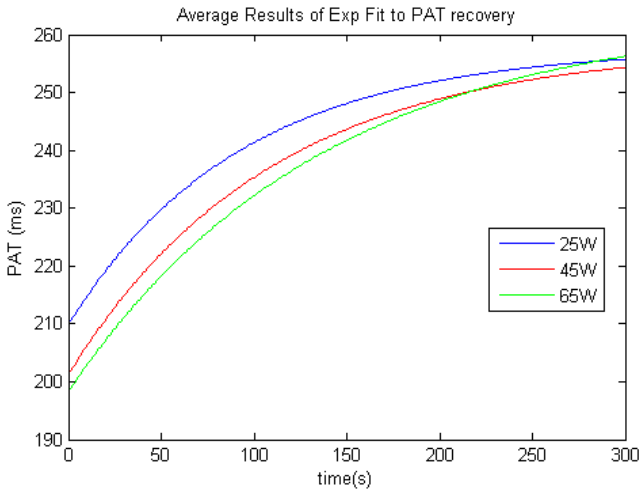

Figure 36 – Graphical representation of PAT recovery exponential equation using average parameter results.

5.3. Patterns of Heart Rate and PAT variation

5.3.1. Typical pattern review

By observing HR as a function of PAT and separating each exercise and recovery runs very similar patterns appeared in almost every subject, exemplified in figure 37.

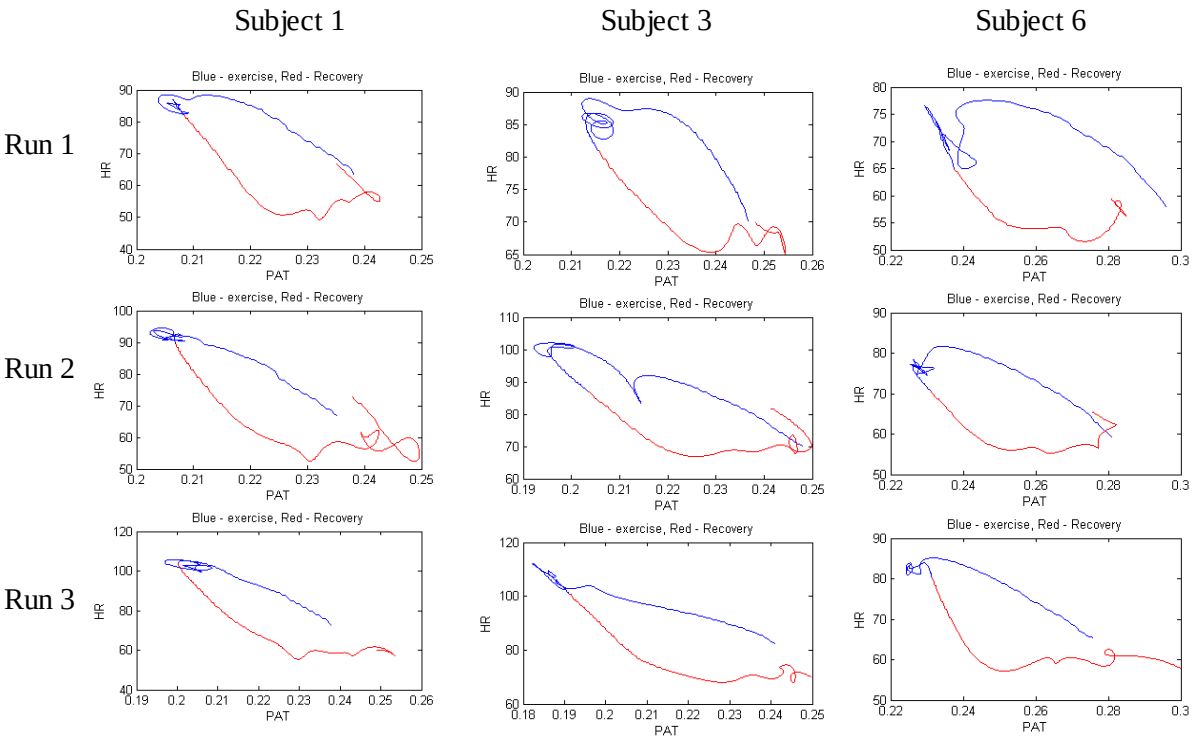

Figure 37 – Pulse Arrival Time vs. Heart Rate for 3 subjects. Exercise (blue) and recovery (red) periods separated: horizontally runs 1, 2 and 3; vertically subjects 1, 3 and 6.

These patterns express a tendency of hysteresis, i.e., the variation path for recovery is not the equal to the one for exercising.

Analyzing the typical variations back to back, there is an example of HR and PAT signals for a subject on figure 38. The same signal and intervals are expressed in a pattern of hysteresis in figure 39. Heart Rate is known to have a small effect on PEP, and similarly on PAT, which is attempted to be removed according to the regression equations of Weissler et al. (1968)[46].

$$PEP' = PEP + 0{,}0004\ HR \quad | \quad PAT' = (PTT + PEP) + 0{,}0004\ HR$$

It was expected that HR variation segments would be more vertical (only HR dependent), and therefore the different events should be more distinguishable (figure 40).

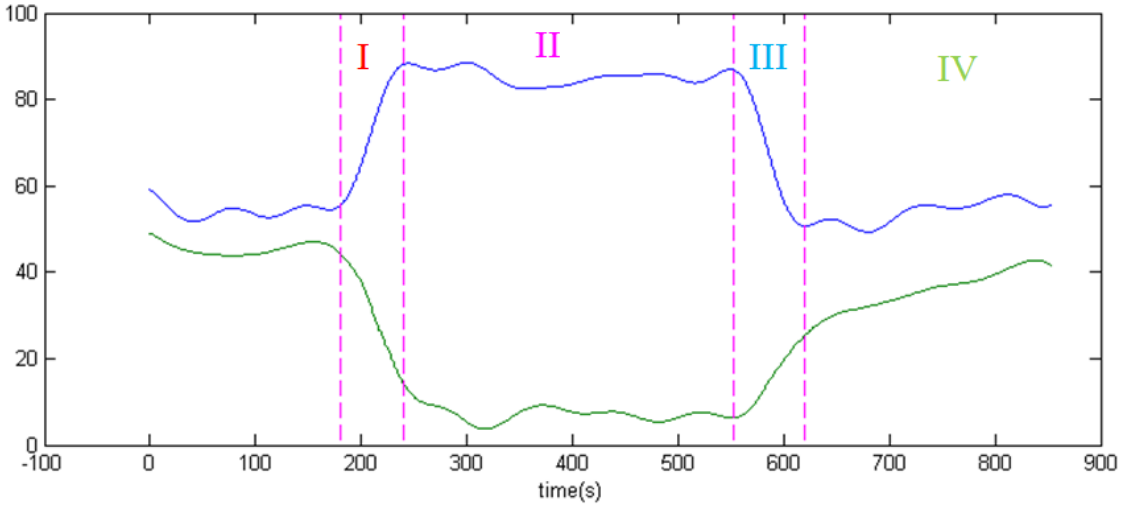

Figure 38 – Example of HR and PAT signals (unscaled) for one subject and one exercise+recovery run with distinction of 4 phases.

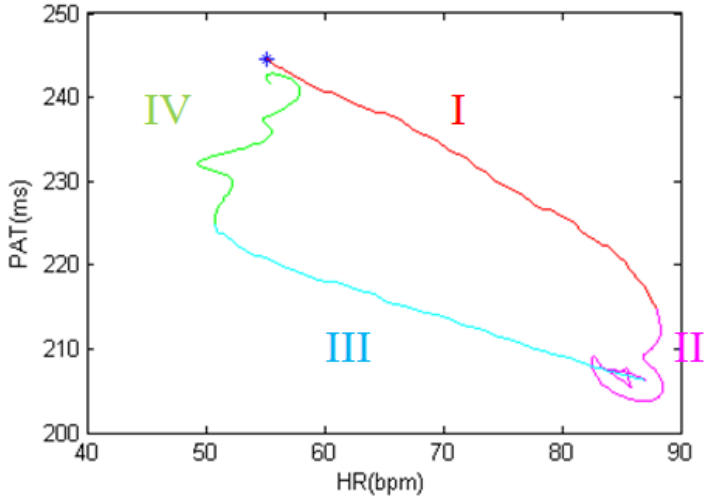

Figure 39 – Pulse Arrival time in order of Heart Rate with 4 phases from same setup as previous figure.

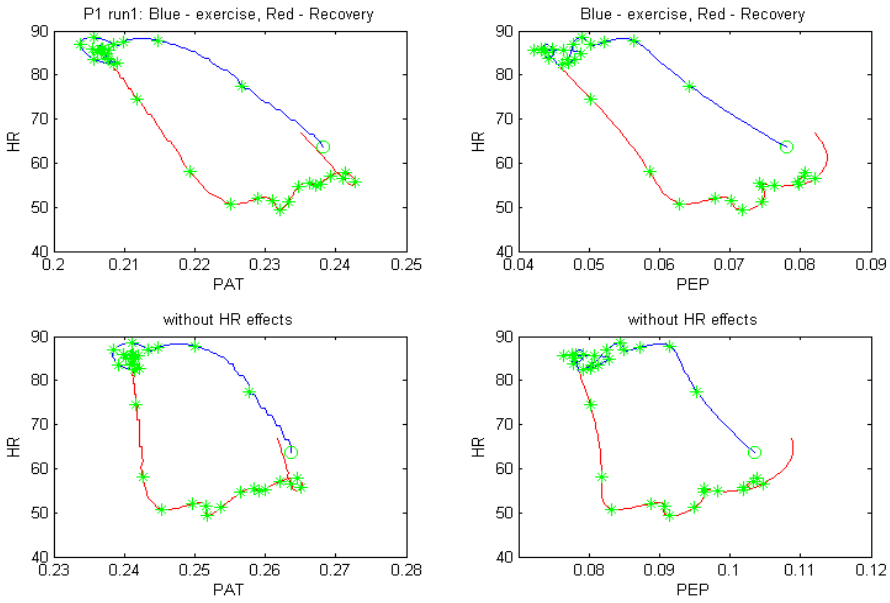

Figure 40 – Pulse Arrival Time and Pre-ejection Period vs. Heart Rate, with or without HR effects, for one patient and one exercise+recovery run. Green markers each 20 seconds, beginning in circumference.

In overall, we observe a clear 4 phase phenomenon:

I. First part of exercising, where HR increases and PEP/PAT decreases almost linearly, and a high state of HR is reached. This lasts approximately 1 minute.

II. Second phase of exercise, where changes are mostly in PAT and PEP. Some patients do not exhibit this phase or the variation is relatively small. It is also the 'bulk' of exercise where HR may suffer slight changes.

III. First part of recovery, where HR returns to a lower state, linearly with PEP and PAT, and seems to be mostly HR dependent when HR effects are taken into account.

IV. Second part of recovery, with almost constant HR, and a long recuperation (increase) of PEP/PAT.

It is very clear for the recovery period the fast action of HR decrease and the delayed PAT/PEP increase. We might relate these events to different regulatory actions in the cardiovascular system. A possible explanation would be fast changes in sympathetic/parasympathetic activity for HR regulation and, with a delayed or slower effect, changes in circulatory resistance or contractility for PAT/PEP, thus the occurrence of hysteresis.

To corroborate the observations, the statistics of slopes of linear fits to each phase are presented in table 7 (averages and standard deviations only, complete statistics in annex 7.2.7).

		I - Onset Exercise				II - Exercise bulk			
		time (s)	dHR/dt	dPAT/dt	dPAT/dHR	time (s)	dHR/dt	dPAT/dt	dPAT/dHR
25W	AVG	59,214	0,373	-0,448	-1,255	304,429	0,011	-0,055	3,063
45W		53,714	0,479	-0,550	-1,233	300,500	0,018	-0,062	-3,279
65W		63,357	0,437	-0,572	-1,356	284,571	0,034	-0,062	0,490
25W	STD	16,244	0,129	0,141	0,314	21,536	0,039	0,041	7,683
45W		7,650	0,131	0,167	0,519	29,763	0,043	0,044	6,040
65W		17,256	0,126	0,162	0,360	42,310	0,041	0,045	10,742

		III - Onset Recovery				IV - Late Recovery			
		time (s)	dHR/dt	dPAT/dt	dPAT/dHR	time (s)	dHR/dt	dPAT/dt	dPAT/dHR
25W	AVG	64,000	-0,372	0,306	-0,950	232,000	-0,010	0,087	3,680
45W		68,857	-0,392	0,344	-0,960	247,071	0,001	0,099	-2,777
65W		72,571	-0,421	0,359	-0,948	255,214	-0,045	0,115	4,915
25W	STD	20,844	0,132	0,094	0,489	28,826	0,091	0,040	9,580
45W		19,187	0,129	0,090	0,360	46,870	0,025	0,047	15,886
65W		26,904	0,142	0,086	0,394	36,722	0,061	0,052	24,624

Table 7 – Average and Standard deviation statistics for linear fits of the 4 stages in exercise+recovery, for each exercise load.

The difference in PAT(HR) slope from the first phase of exercise (I) to the first phase of recovery (III) can be observed although, seen through standard deviations, the values vary a lot depending on subject. The variation rates for HR do not suffer great changes between these two phases, contrarily to PAT variation rates, which are slower for onset recovery. For phases II and IV, PAT variation is still significant and PAT(HR) slopes are highly variable due to different small changes of HR.

5.3.2. Discussion of Special cases

There was an exception in this case, with one subject (subj. 19) exhibiting different patterns of HR and PAT variation, with an almost linear relationship (figure 41).

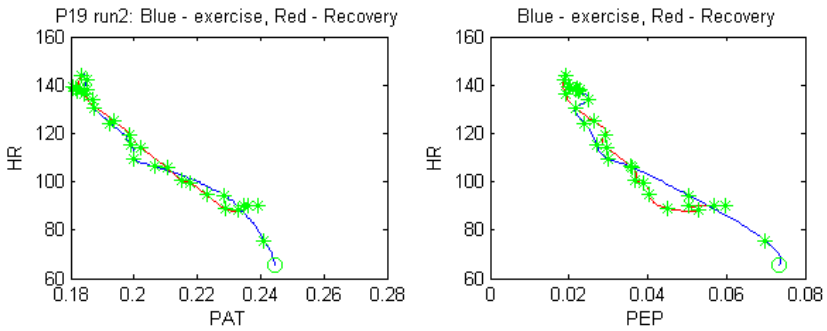

Figure 41 – Pulse Arrival Time and Pre-ejection Period vs. Heart Rate, for subject 19. A different behavior than the usual trend of hysteresis.

No hysteresis is observed, and this occurs also once in subject 20. This unusual behavior is also complemented by an abnormal PPG amplitude behavior in these subjects,

which had relative variations in a much greater order than the rest (figure 42). Their initial PPG amplitude was also much lower. This implies that something different is happening in the cardiovascular system of this subject, which supports the suggestion of, with this kind of analysis, identifying the action of regulation mechanisms and changes in the hemodynamic/cardiovascular status of a subject.

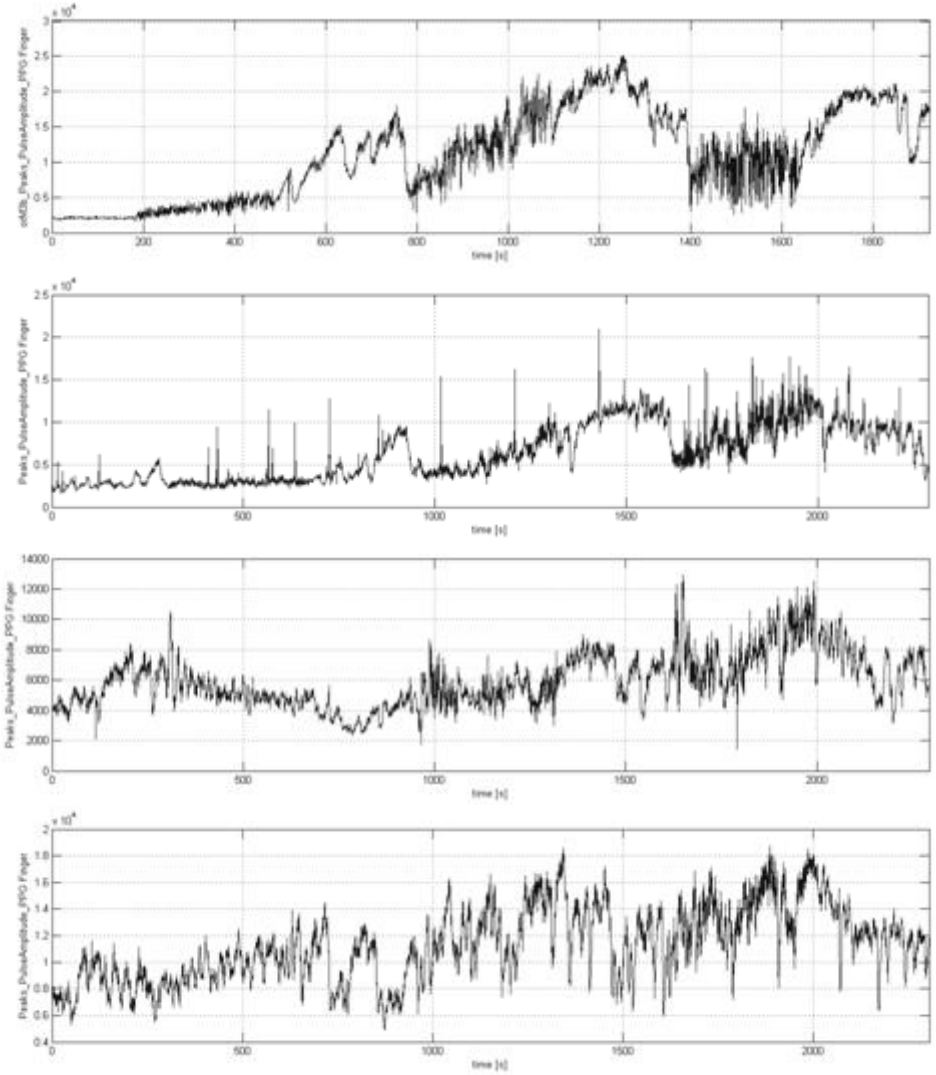

Figure 42 – PPG amplitude evolutions for subjects 19, 20, 6 and 2. Relative amplitude variations from initial state are much larger in subj. 19 and 20.

Several factors affect PPG amplitude, measurements at extremities highly affected by changes in microcirculation. There are other found anomalies of subjects 19 and 20 (seen in subject values from annex 7.2.2):

- they have high exercise HR comparing to the study population. Other 3 subjects also have similar high Heart Rates
- This group of 5 higher HR subjects including 19 and 20 include 2 males and 3 females with the 2 males having the biggest BMIs of the study)
- The group of 5 have a lower exercise Stroke Volume ~ 50ml (study average is 72ml)

- For 19 and 20, Resting Stroke Volume is bigger than for those 3 (~110ml vs. ~80ml); Cardiac Outputs for 19 and 20 are also bigger.

Although being a low sample group with this behavior, they indicate that there is a different cardiac effort and vascular condition. It is the kind of performance closest to what one would expect a debilitated heart would exhibit, such as with congestive heart failure.

6. Conclusions and Future Work

6.1. Main Conclusions (and Contributions)

Pulse transit time did not change with blood pressure for healthy young subjects performing a short-term physical effort test, not showing significant correlation, and a direct or indirect relation could not be achieved. Measurement accuracy of the involved parameters is a big challenge in this setup. Especially obtaining PEP through the ICG provides great uncertainties for the PTT estimation, which may prove to be too large to validate the results. A PEP-free estimation of PTT (DPTT) was derived by using a two PPG setup with improved measurement accuracy compared to the PEP corrected PAT. However, there was also a poor correlation of this measure to SBP, which helps to conclude that the measurement principle may not be the problem, or changes in PTT during exercise, if they occur, are very small and hard to detect. Future applications dealing with PTT should therefore require measurement techniques with improved accuracies.

The applicability of the Moens-Korteweg model, from which calibration functions are derived, is also an issue. The model has strong underlying assumptions, e.g., a nearly constant vessel radius, which might not be valid for elastic arteries of healthy young subjects. For this population it is expected a significant impact on the arterial radius in response to the pressure pulse passage, which could counteract a PTT reduction. Elderly subjects should have more pronounced PTT changes due to their stiffer arteries, less inflicted by radius change.

The proposed heart rate variation model, despite its successful implementation and understanding, was not able to generate a satisfying solution of reproducibility and comparison of behavioral parameters. Nevertheless it promoted a better understanding of neurohormonal response to physical exercise, by recognizing the two moments of regulation mechanisms' action, the fast acting vagal nerve inhibition that may even surpass the needed heart rate (overshoot) and the response of prolonged sympathetic activity leading to a base level of exercising heart rate. On the other hand, linear approaches provide a relatively good numerical description of HR and PAT variations. Exponential approximation to PAT during the recovery period is also a high-quality approach to describe this protocol stage and useful to extrapolate the necessary time for total PAT recovery.

Patterns of HR and PAT/PEP variation easily show the behavior of healthy subjects to these two cardiovascular parameters in physical exercise. There is almost always a behavior of hysteresis, where HR is faster to reach stable levels. This depiction of HR versus PAT may be useful to promptly see the occurrence of deviations to the usual patterns. Deviations in two of the study subjects that also have different behaviors in cardiac function and peripheral blood perfusion lead to conclude that a debilitated heart, the case of congestive heart failure, should exhibit much different variations and patterns.

6.2. Limitations

The low accuracy of available PTT measurements is the main limitation to correctly analyze the PTT alterations through physical exercise. Furthermore, a problem throughout the project is the diminished population sample and it is not possible to say for sure that the observed behaviors happen to all healthy young subjects. Particularly when concluding about some special cases such as subject 19 and 20 in HR versus PAT analysis, it does not have any statistical significance and it is only useful to see what can really happen.

The other major limitation is the non-availability of heart failure data. Having to make do with healthy young subjects, it only allows for an understanding of the methods necessary to analyze the relevant physiological parameters and of usual behaviors. There can only be speculation as to what happens in HF patients and prediction that there will be something different.

6.3. *Future Work*

The performed analysis on healthy subjects sets the base work for a better examination of sick subjects' behavior. The next logical step is to extrapolate the findings to a dataset of heart failure patients and try to find anything that would benefit the evaluation of their recovery from a decompensation episode. Specifically, the predicted tests on HF patients were of medication-induced alterations.

If patient condition is not debilitating, even for coronary artery disease patients, a low-effort exercise test similar to the studied dataset could be performed and direct conclusions to deviations of what is normal would arise.

Furthermore, since elderly subjects usually have stiffer arteries, effects of arterial radius change might be less important and more pronounced PTT variation due to exercise induced BP change might be observable. This could be investigated in further research.

Alternatively, an analysis of syncope (loss of consciousness/fainting) related dataset would be linked to acute alterations in HR and PAT as exemplified in figure 43 from an in-house study, and would be an appropriate follow up to the HR and PAT analysis.

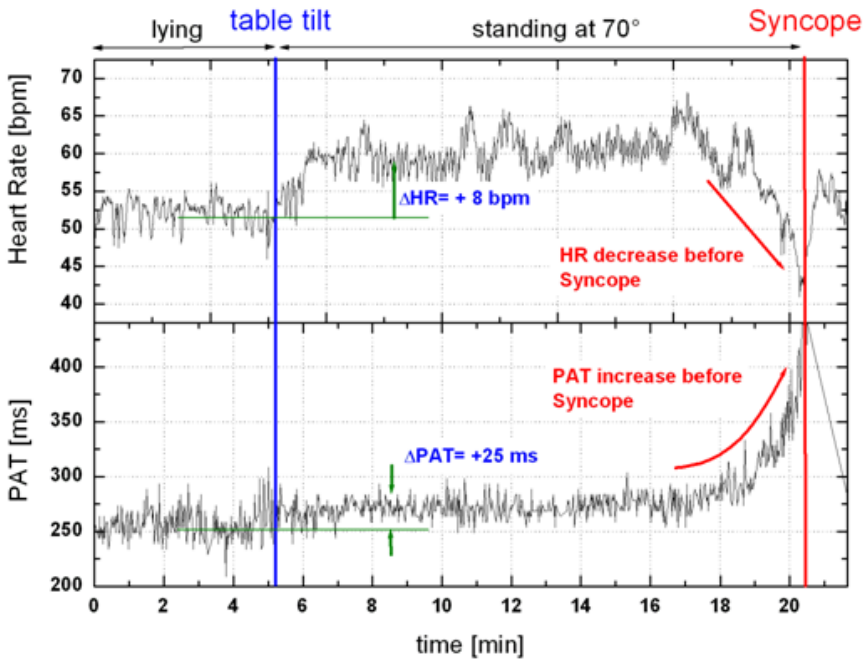

Figure 43 – Example of HR and PAT alterations for a syncope episode induced by posture change.

7. Annexes/ Appendixes / Attachments

7.1. Demonstrations

7.1.1. Moens-Korteweg equation derivation

Consider a cylindrical vessel with a thin elastic wall and a non-viscous fluid, incompressible and perfect, of constant density ρ. This implies that fluid flow is axially symmetric and pressure is uniform in each section of the tube. To reach the M-K equation three different equations are necessary, derived from conservation of mass, momentum along the tube axis and description of wall coupling.

The wall equation is based on the characterization through its Young's elasticity modulus (E), given by a relation of stress and strain. Considering a vessel of wall thickness h and a reference radius r_0, stress σ is the force per unit wall area which is given by the equilibrium of transmural pressure forces ΔP in the tube per unit length from Laplace law [47]:

$$\sigma = \frac{\mathrm{F}}{Wall\ Area} = \frac{\Delta P\, r_0}{h}, \tag{7.1}$$

and strain ε is the relative change in radial dimension, or elongation of circumference wall:

$$\varepsilon = \frac{\Delta r}{r_0}. \tag{7.2}$$

The first equation is achieved by combining the above equations into modulus E:

$$E = \frac{\sigma}{\varepsilon} = \frac{\Delta P\, r_0^{\,2}}{\Delta r\, h} \Leftrightarrow \Delta P = \frac{E\, h\, \Delta r}{r_0^{\,2}} \Rightarrow \frac{\partial P}{\partial t} = \frac{E\, h}{r_0^{\,2}} \frac{\partial r}{\partial t}, \tag{7.3}$$

providing a radius-pressure dependency in terms of wall elastic modulus.

Through conservation of mass, the incompressibility of the fluid implicates that the rate of fluid flow change should be equal to the change of the local element of volume. Given a tube with section S at entrance, velocity υ and element of length dx, the starting fluid flow rate is $Q=\upsilon S$ and the element of volume is $dV=Sdx$. Thus we can have:

$$\frac{\partial Q}{\partial x} = -\frac{\partial V / \partial t}{\partial x} \Leftrightarrow \frac{\partial (\upsilon S)}{\partial x} = -\frac{S\, \partial x / \partial t}{\partial x} \Leftrightarrow S \frac{\partial \upsilon}{\partial x} + \upsilon \frac{\partial S}{\partial x} = -\frac{\partial S}{\partial t} \Leftrightarrow$$
$$\Leftrightarrow \frac{\partial S}{\partial t} + S \frac{\partial \upsilon}{\partial x} + \upsilon \frac{\partial S}{\partial x} = 0. \tag{7.4}$$

By replacing S in terms of radius and resolving, it leads to the similar and equivalent equation:

$$\frac{\partial r}{\partial t}+\frac{r_0}{2}\frac{\partial \upsilon}{\partial x}+\upsilon\frac{\partial r}{\partial x}=0. \tag{7.5}$$

The last terms of equations 7.4 and 7.5 are related to an area gradient which has to be neglected in order to move forward in the derivation of the final solution:

$$\frac{\partial r}{\partial t}+\frac{r_0}{2}\frac{\partial \upsilon}{\partial x}=0. \tag{7.6}$$

Conservation of momentum along the tube is obeyed by the incompressible Navier-Stokes equation:

$$\frac{\partial \upsilon}{\partial t}+\upsilon\frac{\partial \upsilon}{\partial x}=-\frac{1}{\rho}\frac{\partial P}{\partial x}+\nu\frac{\partial^2 \upsilon}{\partial x^2} \tag{7.7}$$

where ν is kinematic viscosity. By dropping the viscosity term (a non-viscous fluid is a condition) and the convection term $\upsilon\partial\upsilon/\partial x$ (laminar flow occurs normally in large and medium arteries which means a low convective acceleration) the necessary third equation is reached:

$$\frac{\partial \upsilon}{\partial t}+\frac{1}{\rho}\frac{\partial P}{\partial x}=0 \tag{7.8}$$

By combining equations 7.3 and 7.6:

$$\frac{\partial r}{\partial t}+\frac{r_0}{2}\frac{\partial \upsilon}{\partial x}=0 \Leftrightarrow \frac{\partial r}{\partial t}=-\frac{r_0}{2}\frac{\partial \upsilon}{\partial x}$$

$$\frac{\partial P}{\partial t}=\frac{E\,h}{r_0^{\,2}}\frac{\partial r}{\partial t} \Leftrightarrow \frac{\partial P}{\partial t}=\frac{E\,h}{r_0^{\,2}}\left(-\frac{r_0}{2}\frac{\partial \upsilon}{\partial x}\right) \Leftrightarrow$$

$$\Leftrightarrow \frac{\partial P}{\partial t}+\frac{E\,h}{2r_0}\frac{\partial \upsilon}{\partial x}=0 \tag{7.9}$$

By differentiating equations 7.8 and 7.9 we have equations 7.10 and 7.11 respectively. In equation 7.11 the term $\partial\upsilon(\partial r^{-1})\partial x\partial t$ is assumed insignificant.

$$\frac{\partial^2 \upsilon}{\partial x \partial t} + \frac{1}{\rho}\frac{\partial^2 P}{\partial x^2} = 0 \tag{7.10}$$

$$\frac{\partial^2 P}{\partial t^2} + \frac{E\,h}{2r_0}\frac{\partial^2 \upsilon}{\partial x \partial t} = 0 \tag{7.11}$$

These two can be combined to achieve the final wave equation from which pulse wave velocity is extracted (PWV=∂x/∂t):

$$\frac{\partial^2 \upsilon}{\partial x \partial t} = -\frac{1}{\rho}\frac{\partial^2 P}{\partial x^2},$$

$$\frac{\partial^2 P}{\partial t^2} + \frac{E\,h}{2r_0}\frac{\partial^2 \upsilon}{\partial x \partial t} = 0 \Leftrightarrow \frac{\partial^2 P}{\partial t^2} - \frac{E\,h}{2r_0}\frac{1}{\rho}\frac{\partial^2 P}{\partial x^2} = 0 \Leftrightarrow \frac{\partial^2 x}{\partial t^2} = \frac{E\,h}{\rho 2r_0} \Leftrightarrow$$

$$\Leftrightarrow \frac{\partial x}{\partial t} = PWV = \frac{\text{distance}}{PTT} = \sqrt{\frac{E\,h}{\rho 2r_0}}, \tag{7.12}$$

the Moens-Korteweg equation.

7.1.2. Derivation of Sensitivity based on Moens-Korteweg

From the Moens-Korteweg and Hughes equations (Equations 4.1 and 4.2 respectively):

$$\frac{PTT}{\text{distance}} = \sqrt{\frac{\rho 2r}{E_0 e^{\alpha P} h}} \tag{7.13}$$

Considering constant radius *r* and wall thickness *h*, having for one individual:

First moment: PTT_0, P_0

Second moment: PTT_1, P_1

$\Delta PTT = PTT_1 - PTT_0$ and $\Delta P = P_1 - P_0$

and dividing PTT_1 and PTT_0, the following can be obtained:

$$\frac{PTT_1}{\text{PTT}_0} = \frac{\text{distance}}{\text{distance}} \sqrt{\frac{\rho 2 r E_0 e^{\alpha P0} h}{\rho 2 r E_0 e^{\alpha P1} h}} \Leftrightarrow \frac{PTT_1}{\text{PTT}_0} = \sqrt{\frac{e^{\alpha P0}}{e^{\alpha P1}}} \Leftrightarrow$$

$$\Leftrightarrow PTT_1 = PTT_0 \sqrt{e^{\alpha(P0-P1)}} \Leftrightarrow PTT_1 - PTT_0 = PTT_0 \sqrt{e^{\alpha(-\Delta P)}} - PTT_0 \Leftrightarrow$$

$$\Leftrightarrow \Delta PTT = PTT_0 \left(\sqrt{e^{-\alpha \Delta P}} - 1 \right), \tag{7.14}$$

which describes a change in PTT in order to a change of pressure P, an initial PTT value PTT_0 and a constant α, effectively allowing an estimation of sensitivity from the accounted models.

7.2. Tables and statistics

7.2.1.

Table 8 – Subject characteristics from the ergometer dataset

Subject	Gender	Age	Height	Weight	BMI
1	m	22	175	65	21,22449
2	m	35	171	70	23,93899
3	m	24	184	82	24,22023
4	f	26	168	54	19,13265
5	f	24	156	45	18,49112
6	m	28	190	85	23,54571
7	m	33	187	80	22,87741
8	m	53	180	70	21,60494
9	f	24	165	60	22,03857
10	m	24	193	95	25,50404
11	m	22	188	87	24,61521
12	m	28	175	66	21,55102
13	f	22	164	49	18,21832
14	m	30	170	70	24,22145
15	f	29	168	53	18,77834
16	m	25	177	68	21,70513
17	m	25	167	72	25,81663
18	m	49	179	80	24,96801
19	f	27	170	55	19,03114
20	m	26	179	90	28,08901
AVG	10m	28,8	175,3	69,9	22,5
STD	4f	8,3	9,8	14,3	2,8

7.2.2.

Table 9 – Subject values for HR through exercise, and high and lows of SV and CO

	low HR	HR 25W	HR 45W	HR 65W	low SV	high SV	low CO	high CO
P1	50	87	92	105	79	115	5,1	9,5
P2	65	98	102	115	81	119	5,6	11,9
P3	65	85	100	110	75	129	7,3	12,1
P4	60	79	89	105	86	119	5,3	11,1
P6	55	70	76	84	102	145	5,9	11
P10	65	83	90	96	96	153	8	14,2
P11	65	80	90	100	95	125	7	13
P13	76	110	126	140	50	70	4,5	9
P15	75	93	122	145	60	85	4,7	9
P16	57	68	80	90	50	90	4,2	7
P17	80	115	118	145	50	80	4,9	10,9
P18	67	84	91	96	76	110	5,8	12,2
P19	61	110	130	150	49	100	5,5	11,1
P20	77	106	118	130	59	112	5,4	12,1
MAX	80,00	115,00	130,00	150,00	102,00	153,00	8,00	14,20
MIN	50,00	68,00	76,00	84,00	49,00	70,00	4,20	7,00
AVG	65,57	90,57	101,71	115,07	72,00	110,86	5,66	11,01
STD	8,86	15,12	17,79	22,59	18,91	23,96	1,09	1,86

7.2.3.

Table 10 – subject values of SBP, PAT, PEP, PTT and DPTT for stages of exercise

	low SBP	SBP 25W	SBP 45W	SBP 65W	high PAT	PAT 25W	PAT 45W	PAT 65W	high PEP	PEP 25W	PEP 45W	PEP 65W	first PTT	PTT 25W	PTT 45W	PTT 65W	first DPTT	DPTT 25W	DPTT 45W	DPTT 65W
P1	120	150	155	175	247	207	204	200	81	45	40	34	163	160	165	168	40	42	39	37
P2	140	165	175	180	243	210	197	187	60	26	21	18	180	181	176	173	59	60	60	58
P3	115	149	156	170	258	212	194	185	87	40	33	29	170	175	165	155	50	60	61	59
P4	125	144	161	167	222	182	175	164	73	36	31	25	148	145	142	136	44	45	54	47
P6	119	144	149	150	301	234	228	225	104	49	45	42	195	189	182	185	69	72	73	69
P10	125	158	155	155	280	243	239	235	90	43	36	32	188	198	205	206	54	57	55	58
P11	140	157	160	169	288	245	241	236	91	58	53	51	195	185	187	187	70	69	71	71
P13	91	147	176	210	238	185	170	167	85	36	26	21	153	148	140	146	39	38	37	35
P15	94	125	150	170	285	231	209	199	98	37	26	20	186	196	180	180	44	42	36	35
P17	96	151	161	200	244	203	190	175	90	30	25	24	152	173	166	150	44	53	52	50
P18	134	149	155	158	250	218	215	210	70	27	27	30	180	185	184	174	49	53	53	52
P19	118	145	134	165	234	181	182	186	80	34	22	18	151	145	160	170	43	44	42	41
P20	129	154	155	157	243	204	202	196	82	27	22	19	155	174	180	180	50	54	56	62
MAX	140,00	165,00	176,00	210,00	301,00	245,00	241,00	236,00	104,00	58,00	53,00	51,00	195,00	198,00	205,00	206,00	70,00	72,00	73,00	71,00
MIN	91,00	125,00	134,00	150,00	222,00	181,00	170,00	164,00	60,00	26,00	21,00	18,00	148,00	145,00	140,00	136,00	39,00	38,00	36,00	35,00
AVG	119,00	149,08	157,08	171,23	256,38	211,92	203,54	197,31	83,92	37,54	31,31	27,92	170,50	173,38	171,69	170,00	50,38	53,00	53,00	51,85
STD	16,42	9,47	10,74	17,27	24,21	21,78	22,63	23,75	11,72	9,45	9,80	10,00	17,70	18,55	18,03	19,14	10,15	10,58	11,95	12,33

7.2.4.

Table 11 – Correlation results for PTT, PAT and DPTT and respective logarithmical calibration

	PTT vs SBP	PTTln vs SBP	PAT vs SBP	PATln vs SBP	DPPT	DPTTln
P1	0,0923	0,0960	-0,7082	-0,7148	-0,1409	0,0804
P2	-0,6213	-0,6255	-0,8179	-0,8252	0,4131	-0,4009
P3	-0,2977	-0,3007	-0,9445	-0,9502	0,1430	-0,1618
P4	-0,7429	-0,7465	-0,8522	-0,8601	0,2563	-0,2456
P6	-0,0102	0,0041	-0,8238	-0,8318	0,5142	-0,502
P10	0,7204	0,7261	-0,9166	-0,9158	0,4126	-0,4088
P11	0,0668	0,0676	-0,8120	-0,8193	-0,0939	0,0995
P13	-0,6996	-0,7011	-0,9086	-0,9195	-0,8281	0,8436
P15	-0,5454	-0,5561	-0,9343	-0,9445	-0,3016	0,2426
P16	0,1507	-0,1362	-0,7918	0,8078	0,2149	-0,2160
P17	0,1704	0,1826	-0,9273	-0,9302	0,6620	-0,6532
P18	0,1908	0,1987	-0,7950	-0,7970	0,6165	-0,6052
P19	-0,6176	-0,6252	-0,6316	-0,6405	0,8488	-0,8196
P20	-0,5712	-0,5431	-0,8810	-0,8839	0,2967	-0,2794
MAX	0,7204	0,7261	-0,6316	-0,6405	0,8488	0,8436
MIN	-0,7429	-0,7465	-0,9445	-0,9502	-0,8281	-0,8196
AVG	-0,1939	-0,2172	-0,8389	-0,8487	0,2153	-0,2162
STD	0,4485	0,4588	0,0905	0,0925	0,4584	0,4286

7.2.5.

Table 12 – A and B parameters from calibration equation fit results to PTT, PAT and DPTT

	PTT		PAT		DPTT	
	A	**B**	**A**	**B**	**A**	**B**
P1	45	228	-143	77	18	88,9
P2	-299	-356	-148	85	-86	446,7
P3	-113	-61	-156	65	-56	310,1
P4	-287	-408	-126	80	-41	276,5
P6	2	133	-124	69	-137	543,8
P10	234	520	-167	66	-96	421,1
P11	48	226	-227	35	66	-29,1
P13	-398	-611	-295	-17	421	-1.229
P15	-283	-341	-182	34	67	-95,6
P17	75	286	-290	9	-224	827,8
P18	37	203	-136	74	-86	398
P19	-181	-208	-153	36	-135	556,3
P20	-77	14	-173	64	-57	306,1
MAX	233,92	520,48	-124,11	84,87	-224,06	827,80
MIN	-398,30	-610,92	-294,65	-17,22	421,28	-1228,70
AVG	-92,10	-28,91	-178,42	52,12	-26,68	217,07
STD	186,62	333,29	57,25	30,73	-157,26	500,59

7.2.6.

Figure 44 – Statistical boxplots for exponential fit of PAT

Boxplot for parameter τ:

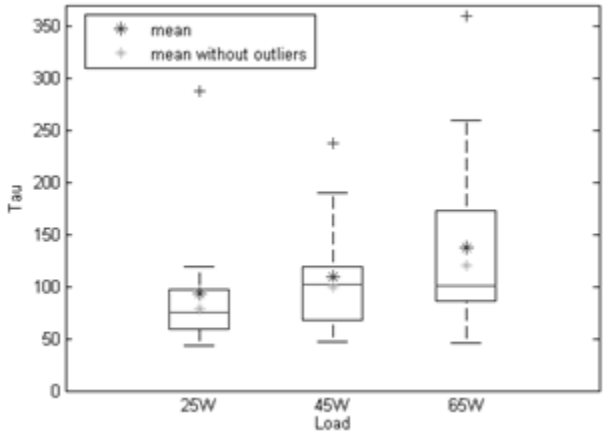

Boxplot for parameter A:

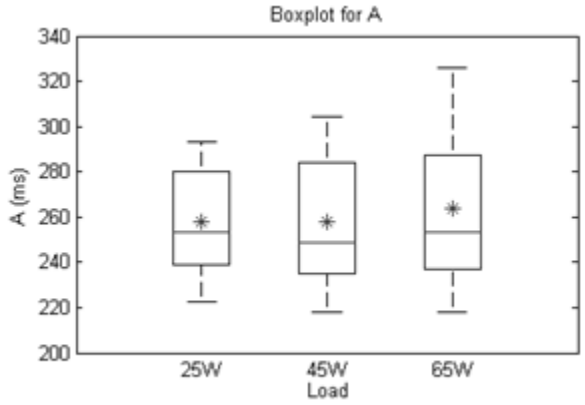

Boxplot for parameter B:

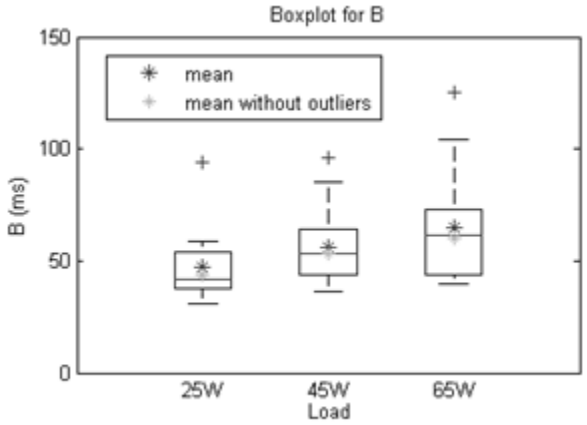

7.2.7.

Table 13 – Linear Fit slopes for HR and PAT

		I – Exercise onset				II – Exercise bulk				III – Recovery onset				IV – Late Recovery			
Run	Subject	time	dHR/dt	dPAT/dt	PAT(HR)	time	dHR/dt	dPAT/dt	PAT(HR)	time	dHR/dt	dPAT/dt	PAT(HR)	time	dHR/dt	dPAT/dt	PAT(HR)
25W	1	61	0,537	-0,488	-0,909	314	-0,003	-0,027	7,963	68	-0,531	0,275	-0,517	235	0,020	0,071	3,525
45W		59	0,538	-0,420	-0,781	314	0,017	-0,031	-1,849	56	-0,536	0,226	-0,423	346	-0,018	0,076	-4,334
65W		56	0,695	-0,532	-0,766	301	0,033	-0,049	-1,480	121	-0,411	0,228	-0,553	264	0,014	0,077	5,327
25W	2	41	0,626	-0,482	-0,769	286	0,010	-0,034	-3,564	51	-0,687	0,215	-0,313	251	-0,313	0,073	4,663
45W		41	0,492	-0,510	-1,038	321	0,045	-0,052	-1,154	61	-0,478	0,238	-0,497	241	-0,005	0,081	-15,528
65W		71	0,404	-0,450	-1,115	291	0,055	-0,065	-1,175	56	-0,590	0,405	-0,687	289	-0,046	0,105	-2,255
25W	3	46	0,352	-0,442	-1,258	316	-0,020	-0,035	1,701	56	-0,275	0,449	-1,633	246	0,017	0,034	1,985
45W		66	0,321	-0,532	-1,656	306	0,012	-0,053	-4,493	66	-0,417	0,446	-1,069	266	0,026	0,082	3,096
65W		104	0,287	-0,502	-1,747	291	-0,001	-0,025	16,346	83	-0,418	0,415	-0,992	278	0,001	0,092	86,682
25W	4	86	0,287	-0,405	-1,410	291	-0,025	-0,018	0,725	81	-0,305	0,263	-0,863	281	0,027	0,052	1,052
45W		66	0,592	-0,608	-1,026	246	-0,064	0,009	-0,135	41	-0,647	0,403	-0,622	341	0,034	0,055	1,641
65W		46	0,466	-0,889	-1,908	261	-0,001	-0,005	4,557	66	-0,436	0,360	-0,826	261	0,012	0,075	6,132
25W	6	51	0,399	-0,667	-1,670	316	-0,007	-0,102	13,754	46	-0,377	0,363	-0,961	251	0,007	0,135	18,429
45W		61	0,387	-0,705	-1,824	311	-0,014	-0,047	3,285	51	-0,370	0,397	-1,072	241	0,023	0,144	6,320
65W		66	0,314	-0,618	-1,969	311	-0,002	-0,032	15,539	46	-0,505	0,298	-0,591	274	-0,011	0,203	-18,423
25W	10	76	0,239	-0,259	-1,083	316	-0,011	-0,039	3,481	46	-0,415	0,080	-0,192	226	0,005	0,134	25,984
45W		46	0,444	-0,182	-0,410	316	0,021	-0,111	-5,272	111	-0,225	0,211	-0,939	211	0,020	0,061	3,082
65W		61	0,321	-0,357	-1,113	331	0,011	-0,059	-5,228	41	-0,647	0,391	-0,605	266	0,007	0,090	13,649
25W	11	51	0,259	-0,389	-1,503	311	-0,003	-0,067	24,145	71	-0,185	0,364	-1,966	231	-0,006	0,048	-7,433

45W		51	0,446	-0,472	-1,058	281	0,004	-0,080	-22,207	91	-0,236	0,261	-1,109	231	0,011	0,115	10,009
65W		66	0,377	-0,541	-1,434	316	0,002	-0,041	-24,707	46	-0,508	0,419	-0,825	269	-0,018	0,112	-6,375
25W	13	56	0,324	-0,380	-1,173	276	0,065	-0,132	-2,032	101	-0,272	0,279	-1,026	181	-0,009	0,107	-12,560
45W		61	0,410	-0,561	-1,368	266	0,068	-0,110	-1,610	66	-0,432	0,433	-1,001	221	-0,010	0,099	-10,310
65W		51	0,448	-0,490	-1,094	211	0,081	-0,112	-1,377	81	-0,308	0,453	-1,471	281	-0,072	0,100	-1,391
25W	15	66	0,383	-0,633	-1,650	256	-0,034	-0,019	0,552	51	-0,319	0,301	-0,943	241	0,036	0,128	3,588
45W		51	0,438	-0,845	-1,930	251	0,062	-0,155	-2,500	56	-0,407	0,510	-1,252	281	-0,040	0,193	-4,817
65W		56	0,560	-0,878	-1,567	251	0,113	-0,171	-1,512	56	-0,573	0,529	-0,923	280	-0,114	0,205	-1,791
25W	16	51	0,334	-0,371	-1,109	336	0,018	-0,032	1,820	51	-0,290	0,275	-0,949	216	0,018	0,057	3,121
45W		51	0,427	-0,408	-0,953	326	0,010	-0,047	-4,804	51	-0,513	0,320	-0,624	236	0,026	0,144	5,508
65W		56	0,486	-0,536	-1,102	311	-0,003	-0,049	16,563	56	-0,483	0,309	-0,641	265	-0,015	0,111	-7,527
25W	17	86	0,190	-0,301	-1,583	311	0,059	-0,081	-1,370	86	-0,482	0,284	-0,590	211	0,074	0,055	0,740
45W		51	0,728	-0,425	-0,584	341	-0,039	-0,067	1,712	66	-0,380	0,378	-0,993	211	0,005	0,103	20,358
65W		96	0,297	-0,400	-1,344	256	0,101	-0,110	-1,087	81	-0,357	0,253	-0,710	254	-0,122	0,184	-1,509
25W	18	76	0,283	-0,407	-1,439	296	-0,010	-0,016	1,590	41	-0,252	0,375	-1,490	261	0,011	0,083	7,410
45W		46	0,304	-0,632	-2,079	311	0,006	-0,032	-5,694	81	-0,187	0,346	-1,847	231	-0,008	0,016	-2,038
65W		51	0,346	-0,488	-1,409	321	0,004	-0,031	-7,045	61	-0,215	0,404	-1,876	243	-0,044	0,044	-0,999
25W	19	41	0,448	-0,315	-0,702	306	0,105	-0,134	-1,273	101	-0,372	0,324	-0,872	176	-0,044	0,166	-3,796
45W		51	0,737	-0,673	-0,913	286	0,104	-0,089	-0,855	91	-0,362	0,319	-0,882	191	-0,049	0,153	-3,095
65W		61	0,615	-0,573	-0,932	201	0,060	-0,097	-1,628	126	-0,239	0,298	-1,247	158	-0,192	0,153	-0,795
25W	20	41	0,561	-0,735	-1,310	331	0,008	-0,035	-4,606	46	-0,449	0,444	-0,987	241	0,016	0,075	4,808
45W		51	0,442	-0,724	-1,638	331	0,019	-0,006	-0,333	76	-0,292	0,324	-1,110	211	-0,001	0,060	-48,774
65W		46	0,503	-0,748	-1,486	331	0,025	-0,022	-0,913	96	-0,203	0,269	-1,324	191	-0,032	0,061	-1,920
Run	Subject	time	dHR/dt	dPAT/dt	PAT(HR)	time	dHR/dt	dPAT/dt	PAT(HR)	time	dHR/dt	dPAT/dt	PAT(HR)	time	dHR/dt	dPAT/dt	PAT(HR)

7.3. *Paper*

Is Pulse Transit Time a good indicator of Blood Pressure changes during short physical exercise in a young population?

Jorge Proença, Jens Muehlsteff, Xavier Aubert, Paulo Carvalho

***Abstract*— The Pulse Transit Time (PTT) is generally assumed to be a good surrogate measure to comfortably track blood pressure (BP) and blood pressure changes. This paper investigates PTT variations for healthy young subjects during a sequence of short-term physical exercises. PTT was measured by two different methodologies having different measurement accuracies as well as underlying assumptions: the total PTT from heart to fingertip and the difference of fingertip and earlobe PTTs. Small non consistent changes and very low correlation of both PTTs with systolic blood pressure (SBP) have been observed for the study population (-0.19 ± 0.45 and 0.22 ± 0.46). In conclusion, there might be a need for an improved measurement accuracy of the sensors and data processing techniques in use. The applicability of the Moens-Korteweg equation is also questionable for young people having flexible arteries. In this case, significant radius changes do occur in the large arteries during exercise, which might counteract a PTT decrease with the BP elevation. These radius effects are exduded from the Moens-Korteweg model.**

I. INTRODUCTION

BLOOD pressure (BP) is one of the most important markers of the cardiovascular system and its beat-to-beat (continuous) monitoring has a high prognostic and diagnostic value for cardiovascular diseases. Non-invasive continuous solutions would highly benefit from an easy and complication-free way towards BP monitoring. Along this line, the Pulse Wave Velocity (PWV) or the inversely related Pulse Transit Time (PTT) have been identified as promising surrogate for comfortable quasi-continuous and non-invasive BP monitoring [1-3]. Calibration steps are necessary to successfully estimate absolute BP from PTT, which have to be robust in terms of significant changes of the cardio-vascular status.

"True" PTT is defined as time of propagation of a pulse to travel a certain distance in a homogeneous arterial segment. To measure a PTT based on this definition at least two transducers have to be placed at the beginning and the end of the arterial segment of interest and the arrival of the pulses have to be detected accurately. For these well-defined situations of short pathways mechanical models have been developed based on fluid dynamic in elastic tubes [1,6]. However, in practice the reliable placement and fixation of two sensors a small distance apart is often difficult and uncomfortable, in particular for home monitoring applications. Therefore, in most of the investigated sensor embodiments for such scenarios the sensors are far apart. Here, pulses propagate through arteries with significant different elastic properties and simple models do not hold. The most common realized embodiment is based on a simultaneous detection of an Electrocardiogram (ECG) and a Photoplethysmogram (PPG) measured from the periphery, since ECG and PPG are easily measurable. However, in this configuration the measured time difference is a Pulse Arrival Time (PAT), which consists of the sum of the entire PTT, i.e. the time interval required for the pulse to propagate from the heart to the PPG sensor location, and the pre-ejection period (PEP), which is not related to pulse propagation.

In this paper, we investigate the relation of PTT to BP measured by two different methods during physical exercise of healthy young subjects. One method is based on subtracting PEP from PAT, where PEP is provided from impedance cardiography. In a second approach we derived a PTT using two PPG sensors with one sensor positioned at the earlobe and the other at a finger. The paper is structured as follows: in section II we describe the experimental setup and the measurement protocol. Section III introduces the prominent Moens-Korteweg model and section IV provides details on the two methods for PTT extraction we used. Section Vpresents the results, which will be discussed in VI.

II. EXPERIMENTAL SETUP

Twenty healthy volunteers were asked to perform a short term physical effort test. Their biometric characteristics were as follows:

- Males/Females: 14 / 6
- Age: 28.8 ± 8.4 years
- Height: 175.3 ± 9.8 cm
- Weight: 69.8 ± 14.3 kg
- Body Mass Index: 22.5 ± 2.8 kg/m^2

The study protocol included an initial phase at rest and 3 sequential sets of physical exercises at 25 W, 45 W and 65 W performed on an ergometer. Each exercise had a duration of 6 minutes followed by a 5 minute recovery period. During the experiment, an electrocardiogram (ECG) and two photoplethysmograms (PPG) placed at the fingertip and the earlobe were continuously obtained at 200Hz. Continuous blood pressure was measured by the Portapres device [4], from which beat-to-beat systolic and diastolic blood pressure values were derived. PEP was provided from an Impedance

This work was supported in part by the EU FP7 project HeartCycle (FP7 – 216695).

J. Proença and P. Carvalho are with the Department of Informatics Engineering, Science and Technology Faculty of the University of Coimbra, Pólo II, Coimbra, Portugal (e-mail: carvalho@dei.uc.pt).

J. Muehlsteff and X. Aubert are with Philips Research Laboratories Europe, Aachen, Germany (e-mail: {Jens.Muehlsteff, Xavier.Aubert}@philips.com).

Cardiograph [5] and breathing effort was monitored via inductive plethysmography (Respiband) sampled at 200 Hz.

Data processing and analysis was carried out with Matlab.

III. Blood Pressure Calibration

A. Moens-Korteweg model

The Moens-Korteweg equation is often employed in blood pressure calibrations, describing the relation between BP and pulse wave velocity. It assumes that the PWV in a short elastic vessel is obtained from its geometric and elastic properties and given by:

$$PWV = \frac{\text{distance}}{PTT} = \sqrt{\frac{Eh}{\rho 2r}} \quad (1)$$

E relates to the elasticity modulus of the vessel wall, h is its thickness, ρ is the density of blood, and r is the radius of the vessel [6]. BP and PWV are interconnected by the relation of elasticity and blood pressure in Hughes equation [7]:

$$E = E_0 e^{\alpha P} \quad (2)$$

where $\alpha \approx 0.017\, mmHg^{-1}$. Pressure in this case is the mean arterial pressure (MAP). The parameters involved in the equations are subject-dependent and not easily measurable. Based on these equations calibration functions can be derived to translate PTT to BP assuming constant vessel thickness and radius. By combining both equations we achieve a logarithmic dependency:

$$P = A \ln PTT + B \quad (3)$$

It should be emphasized that blood pressure is actually regulated by additional factors such as cardiac output, contractility, peripheral resistance and cardiac preload.

B. Model-based PTT-BP Sensitivity estimation

From the Moens-Korteweg based BP model, with the assumption of vessel radius and wall thickness remaining constant, we can derive an equation that relates theoretical changes in PTT to changes in Blood Pressure, i.e.

$$\Delta PTT = PTT_0 \left(\sqrt{e^{-0.017 \Delta P}} - 1 \right) \quad (4)$$

where PTT_0 is known for a given P_0. Using this model, the order of magnitude of expected PTT variations for PTT_0 in the range of 100ms to 200ms accompanied by a change of mean blood pressure of 10mmHg is expected to be about 8-16ms. However, this estimation strongly depends on the parameter alpha and ignores other cardio-vascular changes as, e.g., a diameter change of vessels.

IV. Pulse Transit Time Estimation Approaches

A. Pulse Transit Time with removal of Pre-ejection Period estimated from Impedance Cardiogram

To obtain the "true" PTT we need the time delay between the beginning of ejection of blood due to aortic valve opening and the arrival of the pulse wave at a peripheral location in the arterial system. Within the Impedance Cardiogram the B point of the ICG is assumed to indicate the moment of the aortic valve opening, which is normally used to estimate the pre-ejection period (PEP) as a time difference of the ECG-Q-point and the ICG-B point (PEP extracted by the device is our connection to the B-point; it uses the ECG-R-peak as a reference). Our primary measure Pulse Arrival Time (PAT) is determined by the difference between the R peak of ECG and the foot/onset of the pulse wave of the PPG. By subtracting PEP from PAT we have the estimation of true PTT, i.e.

$$PTT = PAT - PEP \quad (5)$$

Besides a PEP estimation based on the Impedance Cardiogram signal there are alternative methods, such as using heart sounds [10] and echocardiography.

B. Two PPG pulse arrival difference

By using an extra PPG signal in an extremity closer to the heart, which in our case is the earlobe, we extract two distinct pulse arrival moments for every single heartbeat and estimate their difference in time (DPTT). The pulse wave is detectable first at the earlobe and later at the finger and the difference of their arrival time is not affected by PEP. However, this measure is not a PTT for a single vessel as it is assumed for the Moens-Korteweg model, since two arterial pathways – one to the ear and the other to the finger – are involved. If we assume the same mean PWV in both arterial branches and apply the Moens-Korteweg equation, this gives a DPTT of:

$$DPTT = \frac{L_f}{PWV} - \frac{L_e}{PWV} = (L_1 - L_2) \sqrt{\frac{\rho 2r}{E_0 e^{\alpha P} h}} \quad (6)$$

This equation has the same structure as (1) and the calibration function stated in (3) can be applied. The main advantage of using this two PPG method is that it eliminates the need for other signals other than PPG and gives PEP-free measurements.

C. Accuracy of PTT measurements

By obtaining PTT from the subtraction of PEP from PAT, the uncertainty of a PTT measurement accumulates the uncertainties of the estimations of both PAT and PEP.

The measurement error of PAT is determined by the accuracy to detect the ECG-R peak and the robust and accurate detection of a marker in the systolic part of the PPG. In this study the PPG foot point has been used. The detection of the R peak is fairly robust, with an estimated uncertainty of about 2.5 ms, which is half of the 5 ms sampling time. The accuracy of the PPG foot point was determined using a manually annotated dataset of 50 heart beats with estimated accuracy of 4±8 milliseconds. The accuracy of PEP measurements provided by the Niccomo device has been investigated in [8] using echocardiography as reference and was estimated to 9.8 ± 21.4 ms. Using these results the measurement uncertainties appear to be:

$\delta PTT \sim \pm 23$ ms and $\delta DPTT \sim \pm 11$ ms.

V. RESULTS

A. Typical Measurement

Figure 1 presents an example plot of SBP, PTT and DPTT for a complete measurement sequence. At the beginning of the test, when the subject was at rest, SBP was about 140 mmHg with a small decreasing trend, PTT was about 200 ms and DPTT about 75 ms. During exercise systolic blood pressure pronouncedly raises in contrast to diastolic blood pressure (DBP), which did not show significant changes during our short physical effort tests. For constant DBP, mean arterial pressure (MBP) follows the same trend as SBP, however, our analysis focuses on SBP only. Obviously from figure 1, PTT and DPTT neither show a response to SBP nor follow any specific trend, which was consistently observed for all test subjects. There is a large short-term signal variability in PTT as well as in DPTT of up-to 25 ms. This large variance appears also in PAT and correlates well with breathing efforts monitored with the respiration band. This effect has been described in [9].

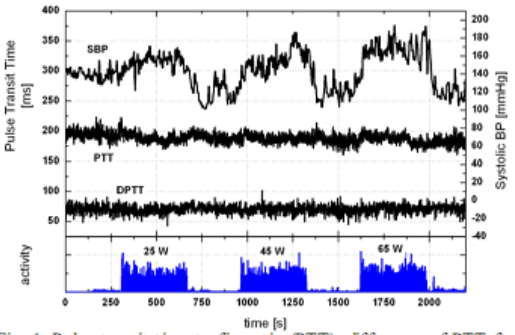

Fig. 1. Pulse transit time to fingertip (PTT), difference of PTT from finger and earlobe (DPTT) and systolic blood pressure (SBP) for complete sequence for one subject. Physical activity periods are also shown. Typically no specific change in PTTs or DPTT could be observed.

B. Statistics, Correlation and Calibration

Table 1 summarizes the average measurement effects for SBP, DBP, PEP, PTT and DPTT for the study population and the different power levels compared to their values at the beginning of the test. Also, we analyzed the linear correlation of PTT, DPTT, and PAT to SBP as well as after a logarithmic transformation. This transformation is marked with (ln). Correlation results are presented in Table 2 as average for all subjects.

Correlations for PTT are generally low, with a high variability, being either positive or negative, whereas theoretically, we expected negative correlation for PTT and positive correlation after a logarithmic transformation. DPTT gave positive correlation with BP, though it is still very low and inconclusive. In contrast, PAT and PATln have a high correlation with SBP during the exercise, where the PATln show a marginal improved correlation.

Based on the calibration function (3) the free coefficients A and B have been determined (table 3), with A being an indicator of the sensitivity of a particular measure to SBP.

For PTTln and DPTTln no consistent values for A could be obtained as it was expected from the correlation analysis, whereas for PATln A is negative, however with a large subject-specific variance.

TABLE I
AVERAGE EFFECTS OF CHANGES OF SBP, PAT, PEP, PTT AND DPTT

	DSBP mmHg	DPAT ms	DPEP ms	DPTT ms	DDPTT ms
25 W	30±13	-45±10	-46±10	1±9	3±4
45 W	39±20	-54±13	-52±11	-1±10	2±5
65 W	54±30	-60±15	-55±12	-3±11	1±5

TABLE II
CORRELATION RESULTS

Variable	Correlation with SBP (average ± standard deviation)
PTT	-0.19 ± 0.45
PTTln	0.22 ± 0.46
DPTT	0.22 ± 0.46
DPTTln	-0.22 ± 0.45
PAT	-0.84 ± 0.09
PATln	0.85 ± 0.09

TABLE III
EQUATION FIT RESULTS: SBP = A LN(VARIABLE)+B

Variable	A (average ± standard deviation [min. – max.])	B (average ± standard deviation)
PTTln	-92 ± 187 [-398 – 234]	-29 ± 333
DPTTln	-26± 157 [-421 – 224]	217 ± 501
PATln	-178 ± 57 [-294 – -124]	52 ± 31

VI. DISCUSSION

Our results suggest that PTT and DPTT are not good measures to monitor blood pressure changes caused by physical exercise in young populations. One explanation might be due to the limited measurement accuracies related to the setups used. The measurement accuracy to extract PEP based on the ICG (9.8 ± 21.37 ms) seems too large in comparison to the expected theoretical 8-16ms PTT change for a 10mmHg BP change. By plotting PTT variation against SBP variation (fig. 2) with the theoretical values from the model (4) including deviations due to measurement uncertainties, we observe that the area between the standard deviation lines covers a very significant part of obtained PTT and SBP variation pairs. This also points to the fact that there may be small PTT variations caused by exercise but we just do not have the necessary sensitivity for correctly detecting them.

With the alternative method, using two PPG at fingertip and earlobe and getting a PEP-free estimation not corrupted by PEP estimation errors, the measured DPTT also did not show a consistent correlation with exercise induced SBP variations. Even though in this case the measurement accuracy is much better, there might be other uncertainties that can make DPTT an unreliable indicator for true PTT.

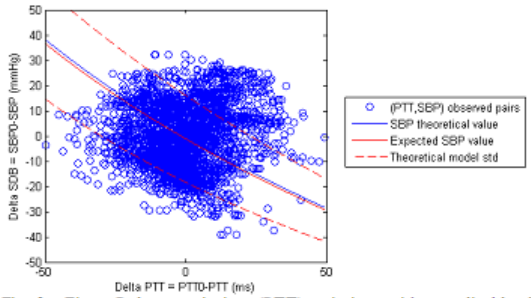

Fig. 2. Finger Pulse transit time (PTT) variations with systolic blood pressure (SBP) variations for the entire study run in one subject, including theoretical expected variations and standard deviations from measurement uncertainties.

Such effects can be related to the two pulse propagation properties for the two distinct arterial pathways.

The validity of applying the Moens-Korteweg (M-K) equation (1) is a topic of discussion as well. This equation has been derived from a simplified mechanical model assuming that there are insignificant variations of vessel radius and section. This may not be true for large arteries as considered in [10-12], especially for healthy young subjects. This population is normally characterized by elastic and compliant arteries, where a blood pressure increase would be accompanied by a larger radius at the passage of the pressure pulse. However, such effects are not taken into account in M-K. Taking pressure dependent changes in radius into account, we can estimate a new sensitivity as in (4), with $\Delta R/R=0.002$ /mmHg in the ascending aorta [13]. This results in expected PTT changes of 5-11ms for a 10 mmHg mean pressure change, representing a 33% decrease compared with the previous 8-16ms. Therefore, considering radius variations should help in obtaining BP, but measuring them would not be sufficiently practical in the uncomplicated, continuous and non-invasive monitoring application we want to address. On the other hand, for stiff arteries typical of older subjects, radius variations would not be as significant, and larger effects on PWV/PTT could be observed. Another variable to be considered is the Cardiac Output, which is not easily accessible non-invasively.

Pulse arrival time (PAT) provided consistent correlation results as was observed before in a similar exercise scenario [14]. High correlation for such experimental settings is mainly due to the prominence of PEP whose effects are not covered by the M-K model at all, which implies to spend more research efforts in physiological responses affecting PEP in order to find suitable calibration function and appropriate – use case scenario specific – monitoring solutions.

VII. Conclusion

Pulse transit times measured by two different methods did not show significant correlation with blood pressure changes for healthy young subjects performing a short-term physical effort test. One essential challenge is related to the measurement accuracy of the parameters used. In particular, obtaining PEP through the ICG provides great uncertainties, which have strong impact on PTT estimation. A PEP-free PTT was derived by using a two PPG setup with improved measurement accuracy compared to the PEP corrected PAT. However, we found also a poor correlation of this measure to SBP, which helps to conclude that the measurement principle may not be the problem, or changes in PTT during exercise, if they occur, are very small and hard to detect. Therefore, future measurements aiming at PTT might require measurement techniques with improved accuracies.

Another aspect is the applicability of the Moens-Korteweg model, from which calibration functions are derived. This model holds under strong underlying assumptions e.g. for a nearly constant vessel radius, which might not be valid for elastic arteries of healthy young subjects. For this population we expect significant impact on the arterial radius in response to the pressure pulse passage, which might counteract a PTT reduction. Since elderly have stiffer arteries, effects of arterial radius change might be less important and more pronounced PTT variation due to exercise induced BP change might be observable. This will be investigated in further research.

References

[1] L. A. Geddes, M. H. Voelz, C. F. Babbs, J. D. Bourland and W. A. Tacker, "Pulse Transit Time as an Indicator of Arterial Blood Pressure", Journal of Psychophysiology, Vol. 18, pp. 71-74, 1981.

[2] B. Gribbin, A. Steptoe and P. Sleight, "Pulse Wave Velocity as a Measure of Blood Pressure Change", Psychophysiology, Vol.13, No.1, pp. 86-90, 1976.

[3] A. Steptoe, H. Smuylan and B. Gribbin, "Pulse Wave Velocity and Blood Pressure Change: Calibration and Applications", Psychophysiology, Vol.13, No.5, pp. 488-493, 1976.

[4] Portapres, www.finapres.com

[5] NICCOMO cardiovascular monitor: www.niccomo.com

[6] Bramwell J. C. and Hill A. V., "The Velocity of the Pulse Wave in Man", Proc. Royal Society for Experimental Biology & Medicine, Vol. 93, pp. 298-306, 1922.

[7] Hughes D. J., Babbs C. F., Geddes L. A., Bourland J. D., Measurement of Young's Modulus of Elasticity of the Canine Aorta with Ultrasound, Ultrasonic Imaging 1, pp. 356-367, 1979

[8] P. Carvalho, R. P. Paiva, R. Couceiro, J. Henriques, M. Antunes, I. Quintal, J. Muehlsteff, X. Aubert, Comparison of Systolic Time Interval Measurement Modalities for Portable Devices, Conf. of IEEE-EMBC, 2010. (submitted).

[9] A. Johannson, C. Ahlstrom, T. Lanne, P. Ask, Pulse wave transit time for monitoring repiration rate; Med. Bio. Eng. Comput (2006) 44:471-478.

[10] Jan Ming-Yie, Hsiu Hsin, Bau Jian-Guo and Wang Yuh-Ying Lin, "One Important Area Gradient Force has been omitted in the Moens and Korteweg's Equation", Proc. IEEE EMBC, pp. 3681-3683, San Francisco, USA, September 2004.

[11] Wang Lin Y-Y, Jan M-Y, Wang G-C, Bau J-G and Wang W-K, "Pressure pulse velocity is related to the longitudinal elastic properties of the artery", Physiol. Meas. 25, pp. 1397-1403, Sept. 2004.

[12] Sola, Josep, Chetelat Olivier and Luprano Jean, "Continuous Monitoring of Corrdinated Cardiovascular Reponses", in Proc. IEEE EMBC, pp. 1423-1426, Vancouver, Canada, August 2008.

[13] J. Greenfield Jr., D. Patel, "Relation between pressure and diameter in the ascending aorta of man" Circ Res. 1962 May;10:778-81.

[14] Muehlsteff J, Aubert X. L. and Schuett M., "Cuff-less Estimation of Systolic Blood Pressure for Short Effort Bicycle Tests: The Prominent Role of the Pre-Ejection Period", IEEE Proc. EMBS, pp. 5088-5092, New-York, USA, 2006.

8. References

[1] European Heart Network - Cardiovascular Disease Statistics 2008

[2] 2005, World Health Organization - http://www.who.int/chp/en/ at 05-02-2010

[3] http://upload.wikimedia.org/wikipedia/commons/thumb/e/e5/Diagram_of_the_human_heart_%28cropped%29.svg/1000px-Diagram_of_the_human_heart_%28cropped%29.svg.png at 16/Jun/2010

[4] http://www.ama-assn.org/ama/pub/physician-resources/patient-education-materials/atlas-of-human-body/circulation-general.shtml at 16/Jun/2010

[5] http://www.benbest.com/health/ECG.html at 16/Jun/2010

[6] Elaine M, Katja H, "Human Anatomy & Physiology, 7th Edition"

[7] Interactive Physiology 9-System Suite, Benjamin Cummings, Pearson Education Inc.

[8] Geddes LA,, Handbook of Blood Pressure Measurement. Humana Press 1991

[9] Geddes LA, Voelz M & Combs C, Characterization of the oscillometric method for measuring indirect blood pressure. Ann Biomed Eng 10: 271–280, 1983

[10] Penaz J (1973) Photoelectric measurement of blood pressure, volume and flow in the finger. Proc. Digest of the 10th International Conf. EMBS, Dresden, Germany: 104.

[11] Boehmer RD (1987) Continuous, real-time, noninvasive monitor of blood pressure: Penaz methodology applied to the finger. J Clin Monit 3(4): 282–287.

[12] Pressman G & Newgard P (1963) A transducer for continuous external measurement of arterial blood pressure. IEEE Trans Biomed Electonics 10: 73–81.

[13] C. Douniama, C.U. Sauter, and R. Couronne, Acquisition of Parameters for Noninvasive Continuous Blood Pressure Estimation – Review of the Literature and Clinical Trial, IFMBE Proceedings 25/IV, pp. 2151–2154, 2009

[14] J. N. Karnegis and W. G. Kubicek, "Physiological correlates of the cardiac thoracic impedance waveform", Am Heart J, vol. 79, pp. 519-523, 1970.

[15] Andreas Bartels and Dietnch Harder, Non-invasive determination of systolic blood pressure by heart sound pattern analysis, Clin. Phys. Physiol. Meas., 1992, Vol. 13, No. 3, 249-256.

[16] M. Y. M. Wong, X. Y. Zhang and Y. T. Zhang, The Cuffless Arterial Blood Pressure Estimation based on the Timing- Characteristics of Second Heart Sound, IEEE-EMBS, 2006

[17] Franchi D, Bedini R, Manfredini F et al. (1996) Blood Pressure Evaluation based on Arterial Pulse Wave Velocity, Proceedings of Computers in Cardiology, Indianapolis, USA, 1996, pp 397–400.

[18] Chen W., Kobayashi T., Ichikawa S., Takeuchi Y., Togawa T., "Continuous estimation of systolic blood pressure using the pulse arrival time and intermittent calibration", Journal of Med. and Biol. Engineering and Computing, Vol. 38, pp. 569-574, 2000.

[19] K.W. Chan, K. Hung and Y.T. Zhang, "Noninvasive and cuffless measurements of blood pressure for telemedicine," in Proc. 23rdAnnu. Int. Conf. of IEEE Engineering in Medicine and Biology Society, Istanbul, Turkey, Oct. 2001, vol. 4, pp. 3592-3593.

[20] C.C.Y. Poon and Y. T. Zhang, "Cuff-less and noninvasive measurements of arterial blood pressure by pulse transit time," in Proc. 27th Annu. Int. Conf. IEEE Engineering in Medicine and Biology Society, Shanghai, P.R.C., 1-4 Sept., pp. 5877-5880, 2005.

[21] Teng X, Zhang Y (2006) "An Evaluation of a PTT-Based Method for Noninvasive and Cuffless Estimation of Arterial Blood Pressure", Proceedings of the 28th Annual International Conference of the IEEE (EMBS), New York, USA, 2006, pp 6049–6052.

[22] Mico Yee-Man Wong, Carmen Chung-Yan Poon, Yuan-Ting Zhang, "An Evaluation of the Cuffless Blood Pressure Estimation Based on Pulse Transit Time Technique: a Half Year Study on Normotensive Subjects", Cardiovasc Eng., 9:32-38, 2009.

[23] US 6,599,251 B2

[24] Poon C et al.,The Effect of Cycling Exercise on Differences in Pulse Arrival Times Measured by a Two Photoplethysmographic Setup, IBHE 2009

[25] J. Muehlsteff, X. Aubert, and M. Schuett, "Cuffless Estimation of Systolic Blood Pressure for Short Effort Bicycle Tests: The Prominent Role of the Pre-Ejection Period", IEEE-EMBC 2006, Vol. 28. pp. 5088-5092.

[26] J. Muehlsteff, X. A. Aubert, and G. Morren, "Continuous Cuff-less Blood Pressure Monitoring based on the Pulse Arrival Time Approach: The Impact of Posture," in Proc.30th Annual Int. IEEE EMBS Conf., Vancouver, British Columbia, Canada, Aug. 2008, pp.1691-1694.

[27] C.C.Y. Poon, Y.T. Zhang and Y. B. Liu, "Modeling of Pulse Transit Time under the Effects of Hydrostatic Pressure for Cuffless Blood Pressure Measurements," in Proc. 3rd IEEE-EMBS International Summer School and Symposium on Medical Devices and Biosensors, U.S.A., pp. 86-89, 2006.

[28] Y. Liu, C. Poon, and Y.T. Zhang, "A hydrostatic calibration method for the design of wearable PAT-based blood pressure monitoring devices," in Conf Proc IEEE Eng Med Biol Soc, Vancouver, 2008, pp. 1308-1310

[29] W. B. Gu, C. C. Y. Poon, H. K. Leung, et al., "A novel method for the contactless and continuous measurement of arterial blood pressure on a sleeping bed", 31st Annual International IEEE EMBS Conference, 2009, pp. 6084-6086.

[30] Villalba E, Arredondo MT, Ottaviano M, Salvi D, Hoyo-Barbolla E, Guillen S, "Heart Failure Monitoring system basedon Wearable and Information Technologies". Journal of Communications, Vol. 2. No. 2, March 2007. Page (s): 10-21. Academia Publisher.

[31] E.Villalba ,D. Salvi, M. Ottaviano, I. Peinado, M. T. Arredondo, A. Akay "Wearable and mobile system to manage remotely heart failure" IEEE Trans Inf Technol Biomed 2009 Jul 28.

[32] http://www.hitech-projects.com/euprojects/myheart/

[33] Portapres, www.finapres.com

[34] NICCOMO cardiovascular monitor: www.niccomo.com

[35] J. Pan and W. J. Tompkins, A real-time QRS detection algorithm. IEEE Trans. Biomed. Eng., BME-32 (3):230-236, 1985.

[36] P. Carvalho, R. P. Paiva, R. Couceiro, J. Henriques, I. Quintal, J. Muehlsteff, X. L. Aubert, M. Antunes, "Assessing Systolic Time-Intervals from Heart Sound: a Feasibility Study", Int. Conf. of the IEEE Engineering in Medicine and Biology Society, 2009

[37] Bramwell J. C. and Hill A. V., "The Velocity of the Pulse Wave in Man", Proc. Royal Society for Experimental Biology & Medicine, Vol. 93, pp. 298-306, 1922.

[38] Hughes D. J., Babbs C. F., Geddes L.A., Bourland J. D., Measurement of Young's Modulus of Elasticity of the Canine Aorta with Ultrasound, Ultrasonic Imaging 1, pp. 356-367, 1979.

[39] P. Carvalho, R. P. Paiva, R. Couceiro, J. Henriques, M. Antunes, I. Quintal, J. Muehlsteff, X. Aubert, Comparison of Systolic Time Interval Measurement Modalities for Portable Devices, Conf. of IEEE-EMBC, 2010. (submitted).

[40] A. Johannson, C. Ahlstrom, T. Lanne, P. Ask, Pulse wave transit time for monitoring repiration rate; Med. Bio. Eng. Comput (2006) 44:471-478.

[41] Jan Ming-Yie, Hsiu Hsin, Bau Jian-Guo and Wang Yuh-Ying Lin, "One Important Area Gradient Force has been omitted in the Moens and Korteweg's Equation", Proc. IEEE EMBC, pp. 3681-3683, San Francisco, USA, September 2004.

[42] Wang Lin Y-Y, Jan M-Y, Wang G-C, Bau J-G and Wang W-K, "Pressure pulse velocity is related to the longitudinal elastic properties of the artery", Physiol. Meas. 25, pp. 1397-1403, Sept. 2004.

[43] Sola, Josep, Chetelat Olivier and Luprano Jean, "Continuous Monitoring of Corrdinated Cardiovascular Reponses", in Proc. IEEE EMBC, pp. 1423-1426, Vancouver, Canada, August 2008.

[44] J. Greenfield Jr., D. Patel, "Relation between pressure and diameter in the ascending aorta of man" Circ Res. 1962 May;10:778-81.

[45] M. Hájek, J. Potůček and V. Brodan, "Mathematical Model of the Heart Rate Regulation During Exercise", Automatica, Vol. 16, pp. 191-195, 1980

[46] A.Weissler, W. Harris, C. Schcoenfeld, "Systolic Time Intervals in Heart Failure in Man", Circulation, Feb 1968; 37: 149 - 159.

[47] Peterson L, Jensen R, Parnell J, Mechanical properties of arteries in vivo. Circ Res 1960; 8(3):622-639.